Technische Universität München
Lehrstuhl für Grünlandlehre

RADOLAN-basierte Erosionsprognose

Franziska Katharina Fischer

Vollständiger Abdruck der von der Fakultät Wissenschaftszentrum Weihenstephan der Technischen Universität München zur Erlangung des akademischen Grades eines

Doktors der Naturwissenschaften

genehmigten Dissertation.

Vorsitzender: Prof. Dr. Kurt-Jürgen Hülsbergen

Prüfer der Dissertation:

1. apl. Prof. Dr. Karl Auerswald
2. Prof. Dr. Annette Menzel

Die Dissertation wurde am 29.01.2019 bei der Technischen Universität München eingereicht und durch die Fakultät Wissenschaftszentrum Weihenstephan für Ernährung, Landnutzung und Umwelt am 31.05.2019 angenommen.

Table of contents

Summary

Introduction: The Universal Soil Loss Equation (USLE) is one among several models which are capable of predicting long-term average soil loss rates. The soil loss rates are calculated as the product of six factors. These six factors account for rain erosivity, soil erodibility, slope length, slope steepness, cultivation management, and permanent erosion control measures. The USLE was first developed and established in the USA and subsequently adapted to conditions in other regions of the World. In Germany, the USLE is used by many federal and state administrative institutions to identify erosion prone sites. However, soil loss predictions by the USLE with institutionally available data have not yet been validated. The lack of validation was due to the great effort to measure soil loss at many agricultural fields over long periods and due to the lack of rain erosivity from rain-gauge data for individual events and individual fields, as erosive rains vary strongly in space and time.

Now, these two deficits could be addressed as contiguous radar rain data with high spatial and temporal resolution have become operationally available from the Deutscher Wetterdienst for Germany, as real-time product (RADOLAN, RADar OnLine ANeichung, radar on-line adjusted) and as radar climatology (RADKLIM, RADarKLIMatologie), both with a resolution of 1 km x 1 km in polarstereographic projection. In principle, weather radars can record all (erosive) rain events at any site. Thus, the spatial and temporal pattern of erosivity can be analysed, even for individual events. Such analyses have not been done comprehensively till now because large data sets of dense rain-gauge networks rarely exist.

In this thesis, it was hypothesized that the availability of RADOLAN and RADKLIM data now allows for calculating rain erosivity and thereby soil loss by the USLE for individual erosion events wherever they occur within the coverage of the radar. It was further hypothesized that the failure to measure these soil losses directly in the fields for validation purposes can be compensated by visual classifications of erosion damages using high quality aerial photos which document the degree of erosion. The visual classifications of erosion damages can

then be used to validate soil loss estimations by the USLE using institutionally available data and RADOLAN derived erosivities.

Indeed, the spatial and temporal resolution of radar rain data is still lower than that of the rain-gauge data. Rain gauges can deliver rain data almost at point scale and typically with 1 min resolution while radar rain data are often available with a resolution of 1 x 1 km² and 5 min or lower. These differences in temporal and spatial scales can affect rain erosivity estimates and hence soil loss estimates. Therefore, erosivities derived from rain data with different spatial and temporal resolutions were compared to determine these scale effects for individual events as well as for the long-term average.

Aims: The main aims of this thesis were to make radar rain data applicable for soil loss predictions and to validate the way at which the USLE is applied by many federal and state administrative institutions. Three main studies were carried out for this: 1) Determining the effects of using RADKLIM data, which have spatial and temporal resolutions lower than the resolution of rain-gauge data, on erosivity estimates. 2) Analysing the spatial and temporal variability of erosivity derived from RADOLAN data. 3) Assessing the validity of soil loss predictions with the USLE using institutionally available data and RADOLAN derived erosivities by visual erosion classifications with aerial photos.

Material & Methods: Rain erosivity is the product of the maximum 30-min rain intensity (I_{max30}) and the kinetic energy of an erosive rain event. A rain event is defined as erosive when it has reached certain minimum thresholds for either total rain depth or I_{max30}. Dry spells of 6 h or longer separate rain events from each other. Annual erosivity is the sum of the individual erosivities of all erosive events within one year.

Aim 1: Numerous large data sets from rain-gauge and radar rain measurements of various spatial and temporal resolutions were analysed to determine the effect of rain data resolution on erosivity estimates. The temporal resolutions varied between 1 min and 120 min and the spatial resolutions between point and 18 x 18 km². Temporal and spatial scaling factors were

determined to correct for the effects of data resolutions lower than 1 min and point scale on erosivity estimates. It was also determined the effect of the difference in method to measure rain by rain gauges and radars on erosivity. This was done at 1 x 1 km² scale with RADKLIM data and with data derived from a dense rain-gauge network. To analyse the effects of spatial scale and method for individual events, the deviations of event erosivity R_e at 1 x 1 km² scale from RADKLIM and R_e at point scale from rain-gauge data were determined.

Aim 2: The spatio-temporal variability was analysed for rain depths and erosivities derived from 5 min RADOLAN data of two years from a study area of ~15 000 km² located in Bavaria. The spatial variability of erosive rain events was determined geo-statistically by semivariogram analyses. Gradients of rain depth and erosivity were calculated by the standard deviation per distance within the range of autocorrelation. The diurnal probability distribution for I_{max30} periods and for dry spells lasting at least 6 h were determined for the temporal pattern of erosive events. Also the diurnal distribution of maximum rain intensities was analysed.

Aim 3: The USLE was validated by comparison of visual classifications of erosion damages and soil loss estimates from the USLE for individual erosive rain events. In total, 8100 fields located in Bavaria were documented by 2500 aerial photos. The photos were taken shortly after erosive rain events had occurred. Each field was visually classified into one out of four erosion classes by a trained person. The visual classifications were tested for reliability by three independent classification repetition runs carried out by trained persons. Values for the USLE factors were mainly taken from the official erosion database of Bavaria and from literature. Erosivities were calculated with 5 min real-time RADOLAN data. The validation of the USLE was done by regression analyses and scatter plots.

Results & Discussion: Annual and event erosivities were increasingly underestimated with decreasing spatial and temporal resolution of the rain data. Accordingly, spatial and temporal scaling factors, which compensate for these underestimations, increased. Temporal scaling factors increased steeper for erosivity at point scale than at 1 x 1 km² scale for temporal

resolutions lower than 30 min. Thus, the spatial scale has to be considered when temporal scaling factors are applied. The underestimation of erosivity based on RADKLIM data compared to erosivity derived from rain-gauge data was a combined effect of resolution and rain measuring method. The method effect accounts for about 24% of the factor to scale annual erosivity derived from 1 x 1 km² RADKLIM to point scale of rain gauges at the same temporal scale. Event erosivities calculated at 1 x 1 km² scale deviate from those at point scale due to the variability of rain within 1 km² that cannot be resolved by these radar data. The direction and magnitude of these deviations vary from event to event. Therefore, the scaling factors are not appropriate for individual events. This contributes considerable uncertainty to event soil loss estimates.

Erosivities of individual events showed strong spatial gradients. These gradients were considerably steeper than those of rain depths. Gradients of erosivity remained pronounced also for annual and biennial erosivities. The biennial erosivity still showed a patchy pattern within the study area. Hence, contiguous, highly resolved rain data are necessary for erosion analyses and far more than two years are required until regional characteristic patterns of erosivity emerge from random scatter which occur in individual years.

The diurnal pattern of erosive events was pronounced. The occurrence of the I_{max30} period followed a diurnal cycle, with a clear peak of occurrence probability in the late afternoon. The timing of this peak agreed with the peak of the diurnal cycle of maximum intensities. Dry spells of at least 6 h between rains were highly common at days with erosive rains and occurred mainly in the morning hours. Mostly, only one of both rain events separated by such dry spells was erosive. Moreover, events often lasted over midnight. Both cases, dry spells separating erosive and non-erosive events during one day and erosive events extending over several days cause rain depths of erosive events to differ from rain depths of individual days. In consequence, temporally continuous rain data should be used for erosivity analyses.

The visually classified erosion damages of the fields agreed well for the different classification repetition runs. Mean soil loss calculated by the USLE increased significantly

with increasing visually classified erosion damage. None of the USLE factors caused directional disagreement between visually classified and calculated soil loss. However, erosivity and erodibility caused less variation in classified and calculated soil loss than the other factors of the USLE. The small influence of erodibility was caused by the narrow range of erodibility in the study area. The small influence of erosivity was rather caused by the difference in spatial scale that still existed even when using radar rain data. The field scale on which soil loss was determined was much smaller than the 1 x 1 km² scale of radar rain data. Large gradients in erosivity within 1 x 1 km² areas, which were already evident from the deviations of erosivity from radar and rain-gauge data for the same event, contributed to the scatter between calculated and visually classified soil loss.

Conclusions: Combining the USLE with radar rain data and institutionally available data allows calculation of valid mean soil loss values for large data sets, and thus also for the long-term. Scaling factors for erosivity have to be applied to compensate for the effects of spatial and temporal resolution and measuring method when using radar rain data.

The high variability of event erosivity within short distances, such as 1 km, is a serious constraint when individual erosion events of individual fields are under focus. Nevertheless, the shown deep spatial erosivity gradients across the total rain cell call for radar rain data in erosion analysis. Their use is promising to allow for more advanced analyses of erosion events instead of using rain-gauge data exclusively. The constraint by the small-scale variability does not apply for long-term mean annual erosivity. This allowed the development of a new map of the R factor for the territory of Germany which can benefit from the advantages of the contiguous and topical RADKLIM data set.

Zusammenfassung

Einleitung: Die ‘Universal Soil Loss Equation’ (USLE) ist eines von vielen Modellen zur Berechnung des langjährigen mittleren Bodenabtrags durch Wasser. Mit der USLE ergeben sich Bodenabtragsraten aus dem Produkt von sechs Faktoren, welche die Bodenerodierbarkeit, das Erosionspotential der Regen (Erosivität), Hanglänge und Hangneigung, Bodenbedeckung und -bearbeitung und permanente Erosionsschutzmaßnahmen berücksichtigen. Das Modell wurde in den USA entwickelt und an deutsche Anbauverhältnisse angepasst. Es wird unter anderem in Behörden genutzt, um erosionsgefährdete Standorte auszuweisen. Jedoch wurde die USLE unter Verwendung der behördlich verfügbaren Daten seit ihrer Einführung in Behörden nicht validiert. Dies liegt zum einen daran, dass langjährige Bodenabtragsmessungen unterschiedlicher landwirtschaftlicher Flächen schwierig und sehr aufwendig sind. Zum anderen war es bisher nicht hinreichend möglich, Erosivitäten mit Ombrometerdaten für einzelne Ereignisse und einzelne Felder zu berechnen. Da erosive Regen meist mit hoher räumlicher und zeitlicher Variabilität auftreten, sind Niederschlagsmessungen nächstgelegener Ombrometer nicht ausreichend repräsentativ für die Fläche der erodierten Felder.

Mittlerweile werden auch flächendeckende, zeitlich und räumlich hochaufgelöste Radarniederschlagsdaten für Deutschland vom Deutschen Wetterdienst (DWD) im Echtzeitbetrieb (RADOLAN, RADar OnLine ANeichung) und als Radarklimatologie (RADKLIM) jeweils mit einer Auflösung von 1 km x 1 km in polarstereographischer Projektion zur Verfügung gestellt. Die Wetterradare des DWD können prinzipiell alle Regen im gesamten Bundesgebiet erfassen. Damit können räumliche und zeitliche Muster der Erosivität auch für einzelne Ereignisse ermittelt werden. Dies war bisher noch nicht umfangreich möglich, da dichte Ombrometermessnetze, welche die Muster erfassen können, kaum betrieben wurden. Mit Radarniederschlagsdaten können nun auch Erosivitäten einzelner Ereignisse und somit auch Bodenabträge einzelner Erosionsereignisse erstmalig unabhängig ihres lokalen Auftretens berechnet werden. Qualitativ hochwertige Luftbilder bieten nun die Möglichkeit, landwirtschaftliche Flächen bezüglich der sichtbaren

Erosionsschäden auszuwerten und somit die Erosionsprognose der USLE, berechnet mit den behördlich verfügbaren Daten, zu validieren.

Die zeitliche und räumliche Auflösung von Radarniederschlagsdaten ist jedoch geringer als die der Ombrometerdaten. Die volumetrischen Radarmessungen liefern Niederschläge gemittelt über eine Fläche von, hier, 1 km x 1 km mit einer maximalen zeitlichen Auflösung von 5 min. Ombrometer können Niederschläge zeitlich hochaufgelöst (typischerweise 1 min) über einer Auffangfläche von meist ~200 cm^2, welche hier als annähernd punktuell betrachtet wird, messen. Die Effekte der zeitlichen und räumlichen Auflösung der Niederschlagsdaten auf die Erosivität wirken sich ebenso auf Bodenabtragsberechnungen aus. Daher ist es notwendig, die Effekte auf die Erosivität sowohl für Einzelereignisse, als auch für langjährige Mittel zu bestimmen.

Ziele: Hauptziel der Arbeit war es, Radarniederschlagsdaten auf ihre Verwendbarkeit zur Prognose von Bodenabträgen zu untersuchen und die USLE, so wie sie behördlich angewandt wird, zu validieren. Dazu wurden drei Studien durchgeführt: 1) Ermittlung der Effekte auf die Erosivität, bedingt durch die zeitliche und räumliche Auflösung und die Messmethodik der Niederschlagsdaten unter Verwendung von Ombrometer- und RADKLIM-Daten. 2) Ermittlung der räumlichen und zeitlichen Variabilität der Erosivität auf Basis von RADOLAN-Daten. 3) Validierung der RADOLAN-basierten Erosionsprognosen unter Verwendung der behördlich verfügbaren Datengrundlagen für die USLE mittels Luftbildauswertungen.

Material & Methoden: Die Erosivität ergibt sich aus dem Produkt der maximalen 30-Minuten-Intensität (I_{max30}) und der kinetischen Energie eines erosiven Regenereignisses. Erosive Regen sind durch einen Mindestwert von I_{max30} oder einer erforderlichen Gesamtniederschlagsmenge definiert. Einzelne Regenereignisse grenzen sich voneinander durch Regenpausen von mindestens sechs Stunden ab. Die Jahreserosivität ergibt sich aus der Summe der Erosivitäten aller erosiven Regenereignisse eines Jahres.

Ziel 1: Zur Ermittlung der Effekte der räumlichen und zeitlichen Auflösung auf die Erosivität wurde eine Vielzahl an Ombrometer- und Radarniederschlagsdatensätzen unterschiedlicher zeitlicher und räumlicher Auflösung verwendet. Die zeitlichen Auflösungen variierten zwischen 1 min und 120 min, die räumlichen Auflösungen zwischen punktuell und 18 km x 18 km. Es wurden zeitliche und räumliche Skalierungsfaktoren ermittelt, um damit die Effekte auf die Erosivität zu korrigieren, die durch Auflösungen geringer als 1 min und punktuell verursacht werden. Weiterhin wurde der Effekt durch die zwei unterschiedlichen Methoden der Niederschlagsmessung, Radar und Ombrometer, ermittelt. Dazu wurden RADKLIM-Daten und Daten eines dichten Ombrometermessnetzes über einer Fläche von 1 km x 1 km verwendet. Zur Bestimmung der räumlichen und messmethodischen Effekte für Einzelereignisse wurden Erosivitäten derselben Ereignisse mit punktuellen Ombrometerdaten und entsprechenden 1 x 1 km² RADKLIM-Daten berechnet und jeweils deren Abweichungen ermittelt.

Ziel 2: Die räumliche und zeitliche Variabilität der Regenmenge und der Erosivität wurde auf Basis von 5 min RADOLAN-Daten eines etwa 15 000 km² großen Untersuchungsgebietes von zwei Jahren ermittelt. Die räumliche Variabilität der erosiven Ereignisse wurde mittels Semivariogrammen geostatistisch analysiert. Die Gradienten der Regenmenge und Erosivität wurden aus der Standardabweichung je Distanzeinheit (km) innerhalb der Distanz, in der Autokorrelation auftrat, berechnet. Zur Charakterisierung des zeitlichen Musters erosiver Regenereignisse wurde die tageszeitliche Verteilung der maximalen Regenintensitäten und der Auftrittswahrscheinlichkeiten von I_{max30} und mindestens sechsstündiger Regenpausen ermittelt.

Zur Validierung der USLE wurden visuell klassifizierte Erosionsschäden mit Bodenabtragsberechnungen der USLE für einzelne erosive Regenereignisse verglichen. Dazu wurden insgesamt 8100 Feldstücke in Bayern mit etwa 2500 Luftbildern ausgewertet. Diese Luftbilder waren kurze Zeit nach dem Auftreten erosiver Regen aufgenommen worden. Jedem Feldstück wurde durch einen Bearbeiter manuell eine von vier

Erosionsschadensklassen zugeordnet. Die Zuverlässigkeit dieser Klassifizierungen wurde durch drei weitere unabhängige Klassifizierungsdurchgänge verschiedener Bearbeiter geprüft. Die Werte für die Faktoren der USLE wurden größtenteils aus der offiziellen Erosionsdatenbank von Bayern und aus der Literatur entnommen. Die Erosivitäten wurden mit 5 min RADOLAN-Daten berechnet. Die Validierung der USLE erfolgte mittels Regressionsanalysen und Scatterplots.

Ergebnisse & Diskussion: Die Ereignis- und Jahreserosivitäten wurden mit abnehmender zeitlicher und räumlicher Auflösung der Niederschlagsdaten zunehmend unterschätzt. Daraus ergaben sich zunehmende zeitliche und räumliche Skalierungsfaktoren. Die zeitlichen Skalierungsfaktoren für Auflösungen geringer als 30 min stiegen für Erosivitäten bei punktueller Auflösung steiler an als bei 1 x 1 km² Auflösung. Daher muss die räumliche Auflösung bei der Verwendung der zeitlichen Skalierungsfaktoren berücksichtigt werden. Die Unterschätzung der Erosivität mit RADKLIM-Daten ergab sich aus einem kombinierten Effekt durch die räumliche Auflösung und durch die Methode der Niederschlagsermittlung aus Radarmessungen. Der Methodeneffekt macht in etwa 24% des Faktors aus, der bei gleichbleibender zeitlicher Auflösung notwendig ist, um die Jahreserosivität ermittelt aus 1 x 1 km² RADKLIM-Daten auf die punktuelle Auflösung zu skalieren. Erosivitäten einzelner Ereignisse auf 1 x 1 km² Auflösung weichen von entsprechenden Erosivitäten auf punktueller Skala ab, da die Radardaten die räumliche Variabilität innerhalb von 1 x 1 km² nicht wiedergeben. Die Stärke und Richtung der Abweichungen ist von Ereignis zu Ereignis unterschiedlich. Diese Abweichungen tragen zur Unsicherheit von Bodenabtragsschätzungen einzelner Erosionsereignisse bei.

Die Gradienten der Erosivitäten von Einzelereignissen waren stark und deutlich ausgeprägter als die Gradienten der Regenmengen. Die Gradienten der Jahreserosivitäten und der zweijährig mittleren Jahreserosivität waren noch ausgeprägter durch die partielle räumliche Überlagerung der Ereignisse. Dies führte zu einem unregelmäßigen Muster der mittleren Jahreserosivität. Die Ergebnisse zeigten, dass flächendeckende

Niederschlagsdaten aufgrund der starken Variabilität der Erosivitäten für die Erosionsforschung notwendig sind und dass Datenreihen von weit mehr als zwei Jahren benötigt werden, bis sich regional charakteristische Muster der mittleren Jahreserosivität aus dem Zufallsmuster einzelner Jahre herausbilden.

Das tageszeitliche Muster erosiver Regen war geprägt durch eine klare Spitze der maximalen Regenintensitäten und der Auftrittswahrscheinlichkeit von I_{max30} am späten Nachmittag. Mindestens sechsstündige Regenpausen zwischen zwei Regenintervallen traten an Tagen mit erosiven Regen häufig und überwiegend in den Morgenstunden auf. Jedoch war meist nur einer der beiden Regen definitionsgemäß erosiv. Weiterhin dauerten Regen häufig über Mitternacht an. Da Regenpausen innerhalb eines Tages erosive von nicht-erosiven Ereignissen trennen und Ereignisse über mehrere Tage hinweg andauern können, unterscheiden sich häufig Regenmengen erosiver Regen und Regenmengen einzelner Tage. Deshalb sollten Erosivitäten mit zeitlich kontinuierlichen Regendaten ermittelt werden.

Die Erosionsklassifizierungen der unabhängig voneinander durchgeführten Wiederholungen stimmten weitgehend gut überein. Der mit der USLE berechnete mittlere Bodenabtrag stieg mit zunehmendem, visuell klassifiziertem Erosionsschaden an. Keiner der USLE-Faktoren verursachte eine gerichtete Unstimmigkeit der berechneten und klassifizierten Bodenabträge. Dennoch zeigten die Scatterplots der berechneten und klassifizierten Bodenabträge weniger Streubreite, wenn die Bodenabträge nach zugehörigen Erosivitäts- und Erodibilitätsfaktoren gruppiert, gemittelt und gegeneinander aufgetragen wurden als wenn gruppiert nach den anderen USLE-Faktoren. Der geringe Einfluss der Bodenerodierbarkeit ergab sich aus der geringen Variation der Bodenerodierbarkeit im Untersuchungsgebiet. Der geringe Einfluss der Erosivität hingegen war durch den Unterschied der räumlichen Auflösung der Feldstücke und der Radarregendaten bedingt. Die Skala der Feldstücke, für welche die Bodenabträge berechnet wurden, war deutlich kleiner als die 1 km² Auflösung der Radarniederschlagsdaten. Dies ließ vermuten, dass starke Gradienten der Erosivitäten innerhalb von 1 km², welche bereits durch die Abweichungen der

Erosivitäten ermittelt aus Ombrometer- und Radardaten derselben Ereignisse aufgezeigt wurden, zu Unstimmigkeiten der berechneten und visuell klassifizierten Bodenabträge führten.

Schlussfolgerungen: Mit Radarniederschlagsdaten und den behördlich verfügbaren Daten liefert die USLE für große Datensätze verlässliche mittlere Bodenabträge. Daher sollten damit auch langjährig mittlere Bodenabträge geeignet geschätzt werden können. Zur Berechnung der dafür notwendigen langjährig mittleren Jahreserosivitäten mit Radardaten müssen jedoch Skalierungsfaktoren angewandt werden, um die Unterschätzung der Erosivität auszugleichen, die durch die zeitliche und räumliche Auflösung und die Methode der Radarniederschlagsermittlung verursacht wird.

Die hohe kleinräumige (≤ 1 km) Variabilität der Erosivität einzelner Ereignisse mindert deutlich die Interpretationssicherheit von Erosionsschätzungen einzelner Ereignisse. Die starken Erosivitätsgradienten über die gesamte Regenzelle hinweg, zeigten dennoch die Notwendigkeit der Verwendung von Radarniederschlagsdaten in der Erosionsforschung. Die kleinräumige (≤ 1 km) Unsicherheit spielt für langjährig mittlere Erosivitäten keine Rolle. Somit wurde eine Neuauflage der Deutschlandkarte für langjährig mittlere Jahreserosivitäten basierend auf Radarniederschlagsdaten ermöglicht. Diese Karte kann von den Vorteilen eines flächendeckenden, 17 Jahre umfassenden RADKLIM-Datensatzes aktuell höchstmöglicher Qualität profitieren.

1 General introduction

Soil erosion is mainly induced by wind and by water. The extent and magnitude of soil erosion by water is larger than by wind, in Europe (Boardman & Poesen, 2003; Verheijen et al., 2009) but also worldwide (Oldeman et al., 1991; Oldeman, 1994). Water erosion occurs in the form of different erosion types depending on the combination of rain, climate, land use, and site conditions. Sheet and rill erosion are the most dominant types of erosion by water (Oldeman, 1994). Erosion of agricultural soils can cause a variety of short- and long-lasting damages. Those damages occur on-site the eroded fields as well as off-site these fields, e.g. in aquatic ecosystems or urban areas (e.g. Auerswald, 1991; Bakker et al., 2007; Carpenter et al., 1998; Pimentel et al., 1995; Stewart et al., 1976; Stoate et al., 2001). A few examples for on-site and off-site effects of erosion are uprooting and coverage of seedlings, reduction of soil fertility, short- and long-term reduction of crop yield, and nutrient and pesticide input into aquatic ecosystems. The temporal and spatial occurrence of erosion events and their magnitude is highly variable (e.g. González-Hidalgo et al., 2009; Steinhoff-Knopp & Burkhard, 2018). This is also true for generally erosion prone areas due to the random and local occurrence of erosive rains, which have certain potential to erode soil, such as thunderstorms (e.g. Lochbihler et al., 2017). Additionally, erosion occurs with high spatial variability within the events, even among replicated plots (Boix-Fayos et al., 2006; Nearing et al., 1999; Rüttimann et al., 1995; Wendt et al., 1986). This small-scale spatial variability of erosion events can be caused by the strong gradients of rain intensities within events (e.g. Fiener & Auerswald, 2009; Lochbihler et al., 2017; Peleg et al., 2013; Renard & Simanton, 1975), among other factors.

In consequence of the high spatio-temporal variability of erosion, it is difficult to quantify soil erosion at field scale under real conditions. Studies have to last several years until the number of erosive rain events affecting a few study sites may be considered large enough for significant findings. Beside this, it is difficult to measure soil loss from fields. The availability of modern, high quality aerial photos might offer the possibility to analyse erosion of recent

events over large areas wherever they occur. The quality of aerial photos may be high enough to visually identify and assess erosion damages at the scale of individual fields. So far, aerial photos were repeatedly used for classification of gully erosion (Castillo et al., 2012; Dymond & Hicks, 1986; Flügel et al., 1999; Grieve et al., 1995), which is comparably easy to identify because of the distinct shape of gullies. They were not in common use to analyse sheet and rill erosion that cause soil losses in the range of only millimetres to centimetres and are hence difficult to quantify visually. The opportunity to use increased quality aerial photos for reliable classification of the severity of erosion in landscapes dominated by sheet and rill erosion deserves examination.

Soil loss has mainly been quantified from plots, as it was practiced at the beginnings of erosion research in the early 20th century. Zingg (1940) initialized the development of soil loss models by relating measured soil loss to site specific conditions. His approach was further developed to the Universal Soil Loss Equation (USLE) which can predict long-term average soil loss (Wischmeier & Smith, 1965, 1978). For an overview of the development of the USLE the reader is referred to e.g. Laflen & Flanagen (2013). The USLE was first developed and established in the USA but it is nowadays applied worldwide (e.g. Lufafa et al., 2003; Park et al., 2010) and well established in Europe (see Boardman & Poesen, 2006) especially for long-term soil loss predictions. Several models are based on the USLE or on factors of it (e.g. Arnold et al., 1998; Cronshey and Theurer, 1998; Foster, 2005; Renard et al., 1997; Young et al., 1989; Van Rompaey et al., 2001; Williams et al., 1983) but also several models based on other approaches exist (see de Vente & Poesen, 2005). For Europe, the models EUROSEM (Morgan et al., 1998) and Erosion2D/3D (Schmidt, 1991; Schmidt, 1996; von Werner, 1995) were developed that follow a different approach and focus on individual events, compared to the USLE which is more concerned with long-term predictions of soil loss. It is the USLE which is used in federal and state administrations to predict long-term mean erosion rates of agricultural fields. These soil loss predictions are especially used to identify those erosion-prone sites for which erosion control measures have to be applied. The institutional application of the USLE was not yet rigorously validated since

its establishment in Bavaria / Germany 30 years ago (Auerswald et al., 1988; Flacke et al., 1990; Neufang et al., 1989a; Neufang et al., 1989b). The lack of validation was due to the difficulty of quantifying amounts of erosion on the long-term to compare them with long-term mean soil loss predictions and due to the fail to use short-term soil loss at field scale because of the lack of rain data with high spatial resolution for short-term soil loss predictions. Nowadays, weather radars are used to obtain rain data spatially contiguously and with high spatial and temporal resolution. Thus, data of rain events are now available for any erosion event that occurs within radar coverage. The Deutscher Wetterdienst provides several different products of radar rain data (DWD, 2018a). Some of them are adjusted to rain-gauge measurements and all have a resolution of 1 km x 1 km in polarstereographic projection. For an overview of the products relevant for this thesis see Chapter 2.2.1. The two best verified radar rain products are the real-time product RADOLAN (RADar OnLine ANeichung, online adjusted radar; Bartels et al., 2004; Winterrath et al., 2012) and the radarclimatology RADKLIM (RADar KLIMatologie) which presently comprises series of 17 years (2001 – 2017) (Winterrath et al., 2017). So far, radar rain data have not yet been widely used in erosion research e.g. to quantify rain erosivity. So, there is the need to examine whether those contiguous radar rain data are suitable for rain erosivity calculations because they might improve erosion analysis significantly.

Rain erosivity is the potential of rain to erode soil and is used as one factor (R factor) in the USLE (Wischmeier & Smith, 1978). The first R factor map for the territory of Germany was developed by Sauerborn (1994) (Fig. 1). She used data and analyses from a number of German studies (e.g. Rogler & Schwertmann, 1981), which determined erosivities according to Wischmeier & Smith using rain-gauge data but mostly sparse in number of rain gauges and limited to measurement series of around ten years (see Sauerborn, 1994). For mapping of point erosivity information, the average annual erosivity was related to long-term average annual or summer rain depth. R factor maps for many other countries, e.g. Italy or Czech (Ferro et al., 1991; Janeček et al., 2013), were developed based on the procedures from Wischmeier & Smith (1978).

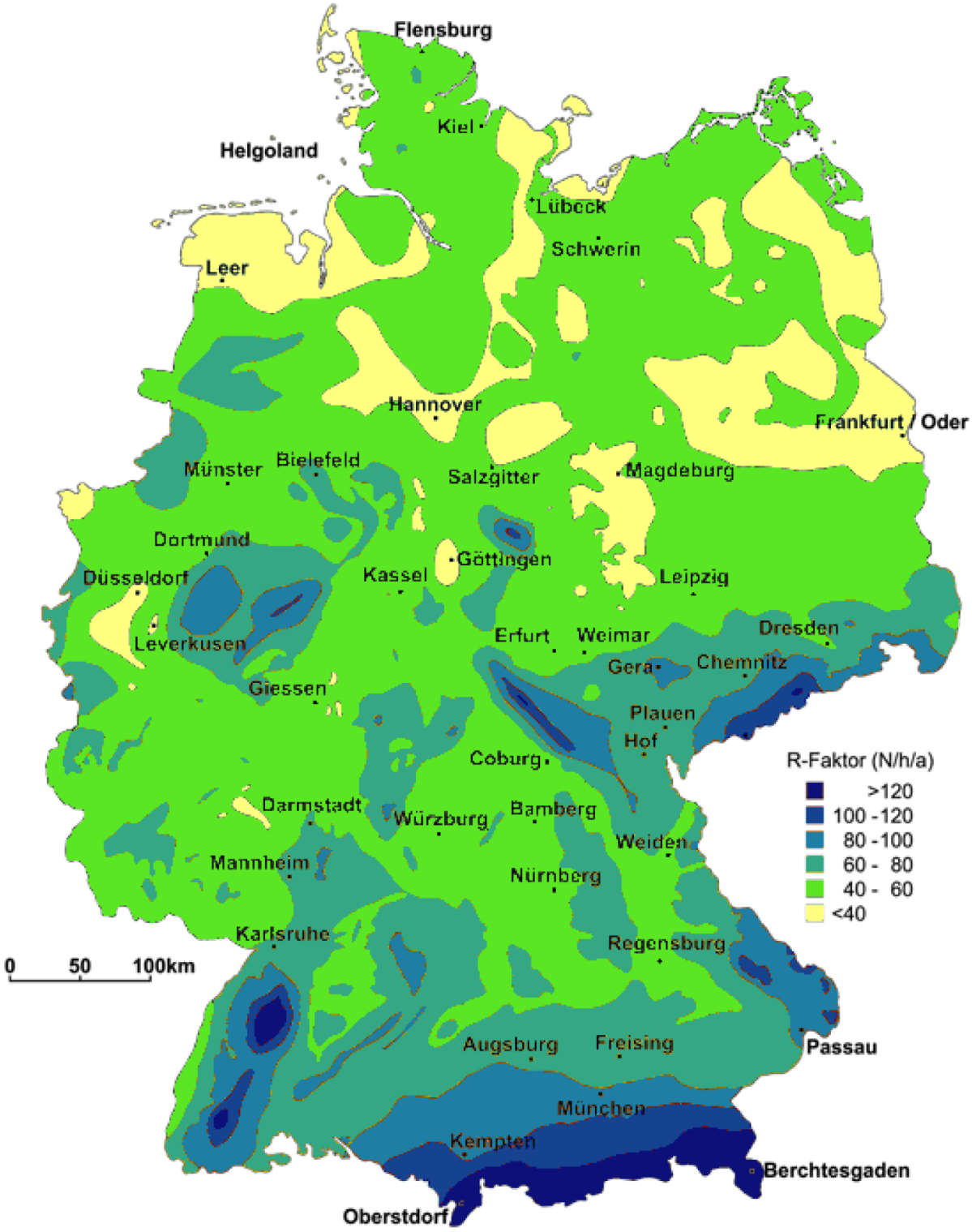

Fig. 1: The R factor map developed by Sauerborn (1994) as published by Auerswald & von Perger (1998) and redesigned by Fischer et al. (2018).

Radar rain data offer major advantages for erosivity calculations due to their spatial contiguous coverage and their relatively high spatio-temporal resolution. Nevertheless, the temporal and the spatial resolution of radar rain data are lower than that of rain-gauge data. Rain gauges can deliver rain data with high temporal resolution (typically 1 min), so almost continuously, over a catch area of usually ~200 cm^2, which is almost point scale. Weather radars deliver rain intensity averaged over the area of a pixel of the radar grid, which is 1 km^2 for most radar rain products of the DWD (DWD, 2018a). Rain intensity can vary considerably already over an area of even 0.5 km x 0.5 km (Krajewski et al., 2003; Pedersen et al., 2010). Therefore, rain intensities and thus also erosivities of individual erosive rain events may differ depending on whether they are derived from rain-gauge data or from corresponding but spatially integrating radar rain data. The direction and the magnitude of these differences may vary from event to event depending on the position of the rain gauge in the radar pixel and the spatial rain pattern. The determination of these differences, here named positional effects, is important for interpretation of soil loss estimates at field scale by either the USLE or aerial photos or other mapping techniques. Therefore, the extent of positional effects needs to be quantified.

In the long-term, positional effects are assumed to level out but erosivity from radar rain data may be underestimated compared to erosivity from corresponding rain-gauge data. This underestimation is assumed to be caused by the lower maximum intensities which apply for the average of a pixel compared to maximum intensities recordable at point scale. This originates from the nature of (heavy) rain cells. Maximum intensities can strongly differ within a rain cell and high intensities are spatially limited to parts of the cell (e.g. Aniol, 1975; Fiener & Auerswald, 2009; Lochbihler et al., 2017; Renard & Simanton, 1975). Erosivity derived from radar and rain-gauge data may also deviate due to the differences in the rain measuring method of rain gauges and radars and their specific limitations (Bartels et al., 2004; Habib et al., 2001; Winterrath et al., 2017). Additional smoothing of the rain data may be caused by the combination of several procedures to finally retrieve rain data from radar measurements.

Typically, the temporal resolutions of radar rain data products are lower than 1 min. Rain intensities can vary strongly from minute to minute and thus, aggregation to time intervals longer than 1 min can cause an underestimation of rain intensity and thus of erosivity. That effect of temporal resolution of radar rain data on erosivity needs to be analysed. This question is important not only for radar data but also for many cases of rain-gauge data where they are available at only low temporal resolution and with fixed intervals. Until today this has only be examined for point rain-gauge data (e.g. Istok et al., 1986; Panagos et al., 2016; Weiss, 1964; Williams & Sheridan, 1991; Yin et al., 2015). The question may even be more difficult to answer in the case of spatially integrated measurements like those by radar because an interaction between the spatial and temporal resolution may occur.

To examine the points raised above, three main studies were carried out which make the vast RADKLIM data applicable for USLE soil loss predictions (Manuscript I), which examine the spatio-temporal pattern of erosive rains in an unprecedented degree of detail (Manuscript II) and which use RADOLAN derived erosivities together with aerial photographs to validate the institutional application of the USLE in Bavaria for the first time since 30 years (Manuscript III).

2 Main material and methods

2.1 Modelling erosion with the Universal Soil Loss Equation

The Universal Soil Loss Equation (USLE) and its successor, the Revised Universal Soil Loss Equation (RUSLE), are the most widely used models in science and in practical applications to predict soil loss. In the following a brief overview of the USLE is given while the details can be found elsewhere (Wischmeier & Smith, 1978; Renard et al., 1997; Foster, 2005). The USLE adapted to German conditions is the model which was introduced to state administrative agricultural institutions. It is known as Allgemeine Bodenabtragsgleichung ABAG (Schwertmann et al., 1990) and the version of its official use (DIN, 2017) is described in Kagerer and Auerswald (1997). This USLE version adapted to German conditions was used throughout the thesis.

The USLE predicts the long-term average annual soil loss A in t ha^{-1} a^{-1} by the product of six factors:

$$A = R \text{ x } K \text{ x } L \text{ x } S \text{ x } C \text{ x } P. \quad (1)$$

The six factors are rain erosivity (R in N h^{-1} a^{-1}), soil erodibility (K in t h ha^{-1} N^{-1}), erosive slope length (L), slope steepness (S), soil cover and crop management (C) and permanent erosion measures (P) (Wischmeier & Smith, 1978). The USLE is based on empirical data of more than 10 000 plot years. The factors L, S, C and P are defined relative to the soil loss of standard plots while R and K have units. The standard plots have a size of 22.1 m x 1.87 m, uniform lengthwise slope steepness of 9% and permanent bare seedbed (Wischmeier & Smith, 1978). For this standard, the dimensionless factors L, S, C and P become 1. The factors differ from 1 when field conditions differ from the standard.

The R factor is the sum of individual event erosivities (R_e) of all erosive rain events n per year averaged over a period of k years (Eq. 2). The sum of R_e of an individual year will be referred to as R_y.

$$R = \sum_{j=1}^{k}\left(\sum_{i=1}^{n} R_{\mathrm{e,i}}\right)_j / k \;\; = \sum_{j=1}^{k} R_{y,j} / k \qquad (2)$$

By definition, erosive rain events require a total rain depth of at least 12.7 mm or a maximum 30-min rain intensity (I_{max30}) of more than 12.7 mm h^{-1} (Wischmeier & Smith, 1978). These thresholds were set to 10 mm and 10 mm h^{-1} for German conditions (Rogler & Schwertmann, 1981). Subsequent events are separated from each other by rain stops of at least six hours. The erosivity of an individual erosive rain event R_e is calculated in N h^{-1} as product of I_{max30} in mm h^{-1} and the total kinetic energy (E_{kin}) of the event in kJ m^{-2} (Eq. 3; Wischmeier, 1959; Wischmeier & Smith, 1958).

$$R_{\mathrm{e}} = E_{\mathrm{kin}} x\, I_{\mathrm{max30}} \qquad (3)$$

The kinetic energy of rain is depending on size and terminal velocity of rain drops. Analyses of drop size distributions of rains were used for relations between kinetic energy and rain intensity *I* (Laws, 1941; Laws and Parson, 1943; Wischmeier & Smith, 1958). For an interval *i* with constant *I*, $E_{kin,i}$ is calculated per mm rain following Eqs. 4.1 – 4.3. The factor E_{kin} in Eq. 3 is the sum of $E_{kin,i}$ of all intervals of the entire rain event.

$$E_{kin,i} = (11.89 + 8.73x\, log_{10}\, I)\; x\; 10^{-3} \qquad \text{for } 0.5 \text{ mm h}^{-1} \leq I \leq 76.2 \text{ mm h}^{-1} \qquad (4.1)$$

$$E_{kin,i} = 0 \qquad \text{for } I < 0.5 \text{ mm h}^{-1} \qquad (4.2)$$

$$E_{kin,i} = 28.33\; x\; 10^{-3} \qquad \text{for } I > 76.2 \text{ mm h}^{-1} \qquad (4.3)$$

Rain-gauge measurements over at least 20 years were recommended by Wischmeier (1959), following Chow (1953), for the analysis of the R factor due to the high spatio-temporal variability of rain and of rain intensities. In comparison, the German standard DIN 19708 requires data series of at least ten years (DIN, 2017). Overall, the minimum period of rain data for the R factor is still discussed (see González-Hidalgo et al., 2009).

Typically, the point information of *R* from rain gauges was transferred to spatial *R* maps by determination of isolines of *R* (lines of equal *R*) using the point information or by relations of *R* to long-term average annual or summer rainfall depth (Rogler & Schwertmann, 1981;

Sauerborn, 1994; Wischmeier & Smith, 1978). In practice, the R factor for soil loss predictions is taken from those *R* maps (e.g. Sauerborn (1994) for Germany, see Fig. 1).

The K factor is defined by the ratio of soil loss to erosivity under standard conditions (Wischmeier et al., 1971). In consequence, the unit of the K factor is t h ha^{-1} N^{-1}. By this, the K factor quantifies the vulnerability of a soil to be eroded. In general, the erodibility increases with decreasing content of organic matter and of sand > 0.1 mm and with increasing content of silt (Wischmeier et al., 1971). Moreover the erodibility increases with soil structure from blocky, platy or massive to very fine granular and with water permeability from rapid to very slow. The K factors under German conditions were first analysed by Martin (1988) and Auerswald (1986a) and later processed by Auerswald & Elhaus (2013) and Auerswald et al. (2014, 2016a, 2016b).

The L factor is the ratio of soil loss per unit area from a field with any length to the soil loss from a field with the standard slope length of 22.1 m under otherwise identical conditions (Wischmeier & Smith, 1978). The S factor is the ratio of soil loss per unit area from a field with any slope steepness to the soil loss from a field with uniform 9% steepness under otherwise identical conditions. Soil loss increases with increasing slope steepness and erosive slope length. The erosive slope length is defined as the length from average starting point of erosion to the position where deposition starts. The curvature of the slope is crucial. Steep gradients in the lower part of a slope promote erosion more than steep gradients in the upper part. In consequence, irregular slopes are subdivided into segments of equal steepness and weighted depending on the position along the slope (Foster & Wischmeier, 1974). The suitability of S factors of the USLE was tested for Bavaria (Germany) by Auerswald (1986b) and procedures were developed to additionally consider the influence of the curvature along and across the slope of the site under focus (Flacke et al., 1990).

In the C factor the relative seasonal distribution of annual rain erosivity and the seasonal variation of the soil loss ratio (c_{SLR}) are combined into a convolution integral of both. The soil loss ratio is defined as soil loss under given surface conditions relative to soil loss from

clean-tilled, continuous fallow under otherwise identical conditions (Wischmeier & Smith, 1978). The soil loss ratio can also be obtained as product of three sub-factors quantifying the effects of green plants, plant residues and land-use related soil properties on soil loss (Wischmeier, 1975). Land-use related soil properties include soil moisture, surface roughness, ridge height, soil biomass, and consolidation. For easy calculation of the C factor from the relative seasonal distribution of annual rain erosivity and the soil loss ratios, the cultivation period of each crop is subdivided into six crop stages, which are mainly defined by soil cover levels. For example, crop stage III comprises the period between 10% and 50% crop cover (Wischmeier & Smith, 1978). The soil loss ratio of each crop stage is multiplied by the relative proportion of annual rain erosivity over the crop stage period. The resulting products of all crop stage periods within a crop rotation are summed up and divided by the number of years of the rotation to yield the C factor. The C factors under German conditions were mainly established by works of Auerswald et al. (1986), Schwertmann et al. (1990), Auerswald & Kainz (1998), Auerswald & Schwab (1999) and Auerswald (2002).

The P factor quantifies the reduction of soil loss by long-term erosion control measures like contouring or terracing relative to soil loss with cultivation up and down the slope and without erosion control measures under otherwise identical conditions (Wischmeier & Smith, 1978). The effectiveness of these measures depends on slope steepness, slope length and crop rotation. For example, contour cultivation is most effective at slopes of 3 - 8% and low or moderate rain erosivities; contour strip-cropping is most effective when strip width and slope length do not exceed certain thresholds which depend on slope steepness (Wischmeier & Smith, 1978). The P values for German conditions were developed by Auerswald (1992) following the methodology used in the RUSLE (Renard et al., 1997).

For soil loss estimation of an individual erosion event A_e, the factor R is replaced by R_e of this individual erosive rain event and the factor C is replaced by c_{SLR} of the respective cultivation and crop stage period in which the rain event occurred (Eq. 5).

$$A_e = R_e \times K \times L \times S \times c_{SLR} \times P \quad (5)$$

2.2 Radar-derived rain erosivity

2.2.1 Measurement and adjustment principles of rainfall

Rain data from weather radar measurements are spatially contiguous, which is the crucial advantage over point rain-gauge measurements. A rain gauge detects only those rain events that occur at its position. That is, for analysis of the extent and intensity gradients of rain events using rain gauges, huge numbers of rain gauges that cover the entire area in which the rain event occurs would be required. In contrast, radars detect rain events area-wide and record their spatial and temporal pattern. This information is of high importance for soil loss analyses.

The procedures to obtain rain data from weather radars are complex. Therefore, there is a continuous development of the individual process steps and a variety of radar rain data products (e.g. Bartels et al., 2004; DWD, 2018a; Helmert et al., 2014; Weigl, 2018; Winterrath et al., 2017). In the following, the measurement principles including some main process steps applied by the Deutscher Wetterdienst (DWD; German Weather Service) are described (Bartels et al., 2004; Winterrath et al., 2017). Information about changes in process steps and weather radar positions between 2008 and April 2018 can be taken from Weigl (2018). Presently, the DWD operates 17 C-band weather radars. Precipitation scans are carried out by these weather radars every 5 min by sending electro-magnetic waves in a frequency of 5.6 GHz (~ 5 cm wavelength) at elevation angles between 0.5° and 1.8° following the orography. Hydrometeors reflect these waves. The signal of the reflection depends on size and number of hydrometeors. The reflectivity measurements of the precipitation scan used for real-time radar rain data products have a resolution of 1° azimuth and 1 km in range and are restricted to a maximum radius of 150 km around each radar station (effective April 2018; DWD, 2018b). The data of all 17 radar stations are merged into a mosaic with a resolution of 1 km x 1 km in polarstereographic projection. Rain depths are derived from the reflectivity measurements by the reflectivity-rain rate ratio (Z-R ratio). The Z-

R ratio varies depending on the drop size distribution of a rain event. Convective and stratiform rain events are distinguished depending on the absolute reflectivity and the horizontal gradient of the reflectivity measurement. For both rain types different drop size distributions are assumed and appropriate standard Z-R ratios are applied.

There are several sources for radar measurement errors. Beside hydrometeors, also flying objects, wind power stations or large buildings reflect radar beams. Those reflections cause clutters due to the high reflectivity from the objects, and cause spokes due to the lack of information in the back of the objects. Attenuation effects are caused by large and heavy rain events but also in general as a result of increasing distance from the weather radar. With increasing distance also the elevation angle of the beam increases. By this, the detection of rain can fail for stratiform rain cells by overshooting of the cell by the radar beam. Moreover, the position of rain measured in the atmosphere and actually fallen to ground level can strongly differ due to wind drift. The degree of error correction differs depending on the radar data product and the version used for data processing. Five different radar rain data products were used in this thesis, namely RY-RADOLAN, RW-RADOLAN, RY-RADKLIM, RW-RADKLIM and YW-RADKLIM (Table 1). These products are described by their main characteristics in the following.

The so called RY products denote rain data which are revised regarding clutters, unrealistic gradients, especially in the overlap area of two radar radii, and regarding orographic shading (DWD, 2018b; Winterrath et al., 2012; Winterrath et al., 2017). The RY data have a resolution of 5 min and 1 km x 1 km in polarstereographic projection covering Germany by a mosaic of 900 km x 900 km, in case of RY-RADOLAN, and 900 km x 1100 km in case of RY-RADKLIM data.

For the reduction of further measurement errors and errors caused by using categorized Z-R ratios, radar rain data are adjusted by rain data of a dense rain-gauge network over Germany. This is implemented in the radar rain data procedure RADOLAN (RADar OnLine ANeichung, radar online adjustment). Presently, rain data of 1200 to 1300 rain gauges (only

~500 in 2005) are automatically sent at least every hour to the data centre of the DWD to use them for the adjustment of radar rain data based on RY-RADOLAN data (Winterrath et al., 2012). RADOLAN data are aimed to be available in real time e.g. for flood forecasting. Therefore, they are available not later than 30 min after the past hour. The realization of this requires a temporal data resolution of 60 min, which then is the temporal resolution of RW-RADOLAN data. RW-RADOLAN and RY-RADOLAN data series start in 2005.

The complete radar data set used for RADOLAN was revised to the climate version RADKLIM (RADarKLIMatologie; radar climatology) by additionally using of historical quantitative radar data to prolong the series back to 2001 and by using hourly and daily data of up to 4401 rain gauges in total (Winterrath et al., 2017). The radar data were restricted to the radius of 128 km around the weather radar respectively to ensure uniformity throughout the series beginning in 2001. In case of version 2017.002, the radar data were corrected for decreasing signal power with increasing distance from the weather radar using developments based on the approach of Wagner et al. (2012). Spokes were corrected based on the method of Jacobi et al. (2014) and further artefacts were corrected by several different approaches (see Winterrath et al., 2017). The RW-RADKLIM product is based on RY-RADKLIM data and has a resolution of 60 min and 1 x 1 km² in polarstereographic projection covering Germany by a mosaic of 1100 km in North-South and 900 km West-East direction for the period from 2001 to 2017 (Winterrath et al., 2018a). Recently so called YW-RADKLIM data with a temporal resolution of 5 min became available (Winterrath et al., 2018b). This product is basically RY-RADKLIM data, which are indirectly adjusted to rain-gauge data. The twelve 5 min RY data which spatio-temporally correspond to one rain-gauge-adjusted 60 min RW-RADKLIM data are multiplied by the ratio of the RW data to the sum of the twelve RY data.

Tab. 1: Characteristics of the radar rain data products of the Deutscher Wetterdienst (Bartels et al., 2004; DWD, 2018a; Winterrath et al., 2017) which are relevant in this thesis. Here, all RADOLAN products cover a mosaic of 900 km x 900 km and all RADKLIM products cover a mosaic of 1100 km x 900 km over Germany. All these products have a spatial resolution of 1 km x 1 km in polarstereographic projection.

Product name	Temporal resolution	Rain-gauge-adjusted	Maximum radar radius (km)[2]	Quality controlled[3]	Correction for (orographic) shading	Correction for spokes	Used in manuscript
RY-RADOLAN	5 min	No	128/150	Yes	Yes	No	II, III
RW-RADOLAN	60 min	Yes	128/150	Yes	Yes	No	II, III
RY-RADKLIM	5 min	No	128	Yes	Yes	Yes	I
RW-RADKLIM	60 min	Yes	128	Yes	Yes	Yes	I
YW-RADKLIM	5 min	Yes[1]	128	Yes	Yes	Yes	I

[1] YW-RADKLIM data are based on RY-RADKLIM data and indirectly adjusted to rain-gauge measurements by RW-RADKLIM data
[2] Maximum radius of radar measurements used for composite generation; for RADOLAN products, the radius was changed from 128 km to 150 km in 2010
[3] Including statistical suppression of clutters and smoothing of gradients

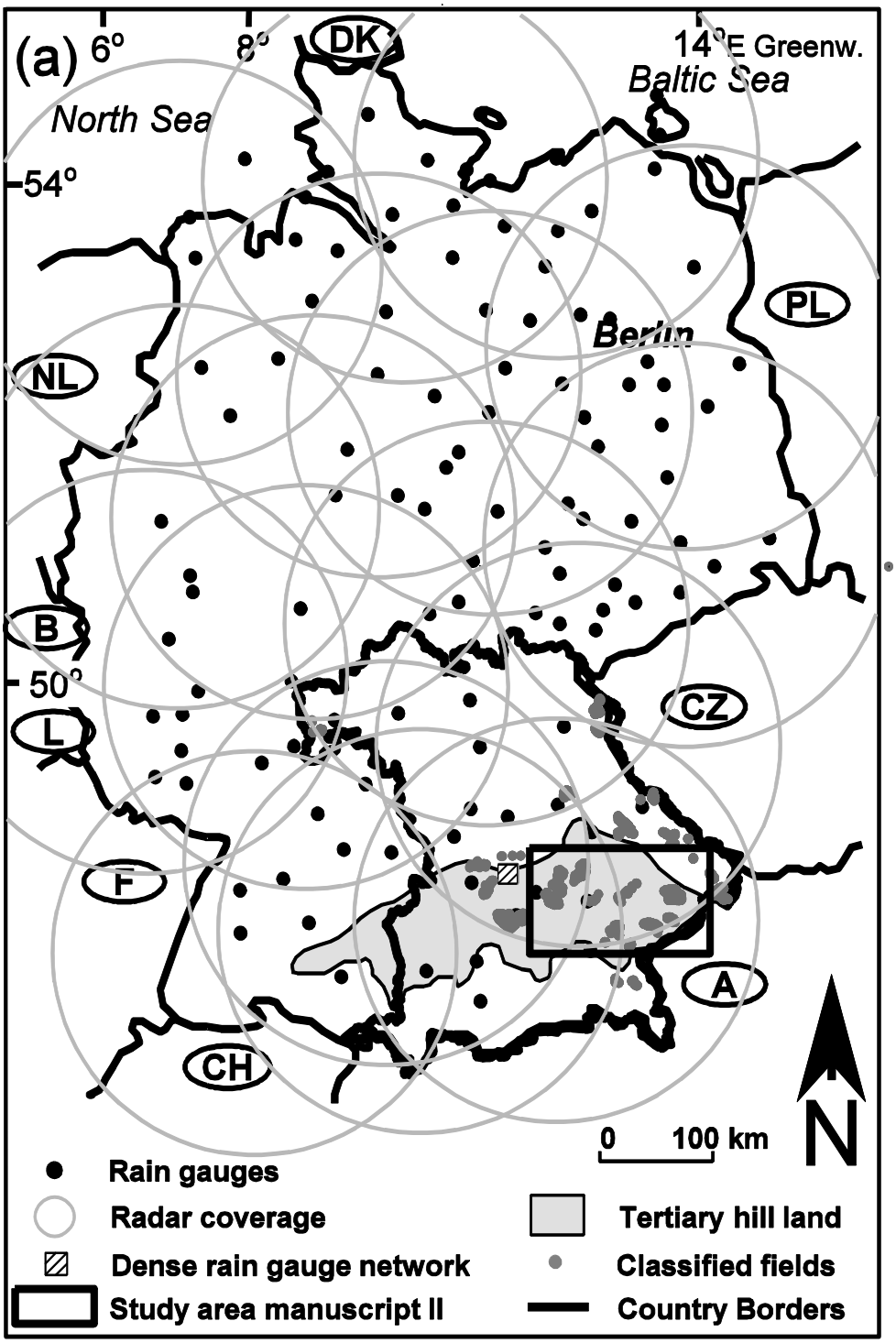

Fig. 2: Illustration of the radar coverage of the 17 weather radars across Germany operated by the Deutscher Wetterdienst (grey circles). Distribution of rain gauges (black dots; size exaggerated) and location of the dense rain-gauge network over 1 km x 1 km (hatched square; size exaggerated) used for determination of scaling factors in Manuscript I. Location of the study area (rectangle) used in Manuscript II for determination of the spatio-temporal pattern of erosive rains. Illustration of the locations of the 8100 fields (grey dots; size exaggerated) used for validation of the Universal Soil Loss Equation in Manuscript III. The fields were mainly situated in the Tertiary hill land (highlighted in pale grey), an erosion prone area in Bavaria (southeast Germany).

2.2.2 Effects of temporal and spatial scale and rain measurement method on erosivity

Calculations of erosivity with (radar) rain data of resolutions lower than point scale and lower than 1 min result in an underestimation of erosivity. This underestimation arises from the underestimation of local intensity with decreasing temporal and spatial resolution of rain data and hence the underestimation of I_{max30}. In consequence, the I_{max30} minimum threshold which defines events to be erosive is exceeded by less rain events. The threshold for I_{max30} was adjusted in that way to not underestimate the number of erosive events with data of temporal resolutions lower than 1 min. Total rain depth, in contrast, is not affected by the temporal resolution so that the threshold for event rain depth remained unchanged. In comparison to event number underestimation due to low temporal resolutions, event number underestimation due to low spatial resolutions is not only caused by underestimation of I_{max30} but also by the lower occurrence probability of dry spells of 6 h or longer. The probability for absence of rain in the total pixel decreases with increasing pixel width so that the probability that two rains are defined as one rain event increases with increasing pixel size. Therefore, the minimum thresholds were not adjusted for the effect of spatial resolutions lower than point scale. Any difference in the number of events at point scale and at lower resolutions is included in the spatial scaling factor.

Spatial scaling factors were determined basically by the ratio of annual erosivity derived from data of highest spatial resolution to annual erosivity derived from data of lower spatial resolution. The spatial scaling factors were determined with several rain-gauge and RADKLIM data sets covering mainly up to 16 years with resolutions between point scale and 18 km x 18 km. Rain data with resolutions > 1 km^2 were generated by spatial integration of RADKLIM data. The effect on erosivity caused by the method to measure rain either by rain gauges or by radars was determined by the difference in the spatial scaling factors as derived at 1 x 1 km^2 scale from RADKLIM data and from spatially integrated rain-gauge data.

The spatially integrated rain-gauge data are generated from rain data of the dense network of 12 rain gauges (see Fig. 2). These data are referred to as ‘pseudo-radar’ data.

For individual events, the deviation of R_e from 1 x 1 km² (pseudo-) radar data and from rain-gauge data is depending on the position of the rain gauge within the (pseudo-) radar pixel and the pattern of the rain. This ‘positional effect’ varies from event to event. It was quantified by the ratio of R_e at point scale and R_e at 1 x 1 km² scale separately for events with R_e at point scale larger and lower than R_e at 1 x 1 km² scale. The same procedure was followed for R_e at point scale and R_e at 0.5 x 0.5 km² scale using the pseudo-radar data set.

The effect on R caused by temporal resolutions lower than 1 min was determined with 1 min rain data from rain gauges covering series of 16 years respectively. These data were aggregated to 2 min, 5 min, 10 min, 15 min, 30 min, 60 min, 80 min, 100 min, and 120 min resolution. Erosivities were calculated with data of each temporal resolution considering the adjusted I_{max30} thresholds. The temporal scaling factors resulted from the average ratio of R derived from 1 min data to R derived from data with temporal intervals > 1 min. On the same way, temporal scaling factors were derived at 1 x 1 km² scale from 5 min YW-RADKLIM data over 16 years.

The robustness of the factors and the effects was given by their 95% confidence intervals (CI). All calculations were done in program R version 3.2.0 and higher (R Core Team, 2015).

2.2.3 Spatio-temporal variability of erosivity

The spatio-temporal variability of erosivity was determined by radar rain data of an area of 86 km x 181 km located in southern Germany (see rectangle in Fig. 2) covering the years 2011 and 2012. RY-RADOLAN data were indirectly adjusted by RW-RADOLAN data as such rain-gauge-adjusted 5 min radar rain data were not available as real-time product from the Deutscher Wetterdienst at the time when the present study was conducted. Erosivities were calculated as described in Chapter 2.1 by Eqs. 2, 3 and 4.1 to 4.3. The scaling factors were

not applied as they are not adequate for individual events but only for robust mean annual erosivities which require data series over at least ten years (DIN, 2017). Importantly, correction by scaling factors is not necessary in the case of this study because they do not affect the relative spatial gradients and the temporal pattern of erosivity. RW-RADOLAN data were verified by independent rain-gauge measurements.

The spatial variability was geostatistically analysed for daily rain depths, E_{kin}, I_{max30}, R_e, R_y, and R as biennial average of R_y by semivariograms using gstat (Pebesma, 2004) in program R version 3.2.0 and higher (R Core Team, 2015). Theoretical semivariograms were fitted to the experimental semivariograms. Nugget, sill and range were determined by the theoretical semivariogram (see Fig. 3 for an example of a semivariogram). The partial sill results from the sill minus the nugget. Gradients of rain depth and R_e were described by the square-root of the variance (partial sill) in relation to the range of autocorrelation. The relative gradients were determined by the gradients related to mean rain depth and R_e respectively. Additionally, short-distant gradients within 1.4 km were determined.

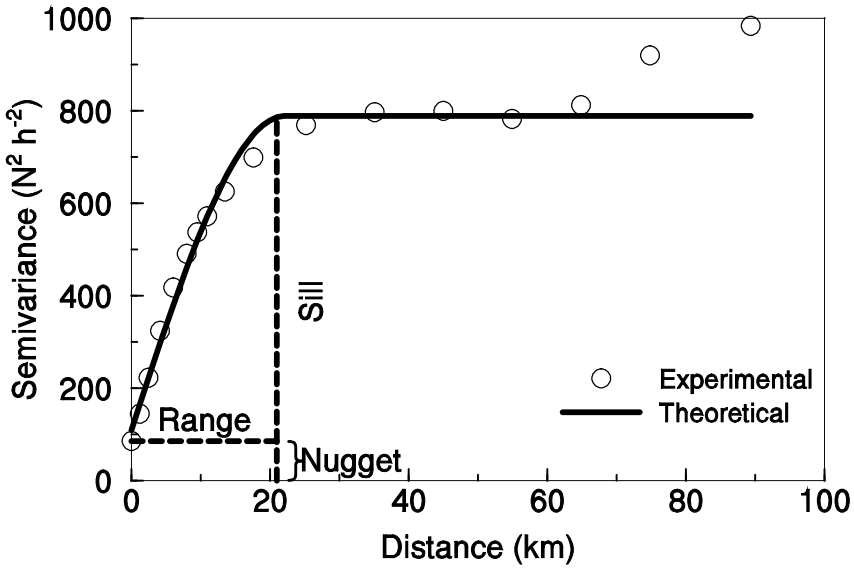

Fig. 3: Experimental semivariogram (points) and theoretical semivariogram (line; here: spherical model), here for the erosivity of an event, with the distance of autocorrelation (range), the maximum semivariance (sill) and the nugget, which accounts for local scatter and measurement errors.

The diurnal probability distribution for the occurrence of dry spells of 6 h or longer and for the occurrence of I_{max30} was used to characterize the temporal pattern of erosivity. For this, the kernel density estimation was taken (Silverman, 1986). Additionally, the diurnal pattern of maximum rain intensities was determined. The pattern within the strong variability of intensities was filtered by the 98 percentile of intensities within a window of 120 min width moving in 5 min steps.

2.3 Validation of the USLE adapted to Bavarian conditions using radar-derived erosivities and aerial photos

The adapted version of the USLE was validated by the comparison of visually classified and calculated soil loss of 8100 fields located in Bavaria, southern Germany (see grey dots in Fig. 2).

The aerial photos of the fields were taken in 2011 and 2012 shortly after prominent rain events were recognized in any erosion prone area in Bavaria. For an example of such an aerial photo documenting considerable erosion damages see Fig. 4. Each documented field was assigned manually by a trained person into one of four soil loss classes. Class 0 was assigned to fields without visible erosion features. Class 1, 2 or 3 was assigned when <10%, 10-30% or >30% of the field area showed erosion features such as rills (for examples of the four classes see Figure A1 in the supporting information of Manuscript III). Each of the 8100 fields was classified at least once or up to four times by three different trained persons. Based on all fields with at least two classifications, the classifications were evaluated for conformity by regression analysis and the Nash-Sutcliffe efficiency (Nash & Sutcliffe, 1970).

Fig. 4: Aerial photograph documenting erosion damages at agricultural fields after the occurrence of erosive rain events. The aerial photo was taken by Wolfgang Bauern.

The soil loss of all erosive rain events between the last tillage and the day of taking the aerial photo of a field were calculated according to Eq. 5 and summed up. The factor R_e was calculated using 5 min RY-RADOLAN data indirectly adjusted by the corresponding RW-RADOLAN data of the certain area and period. This adjustment procedure was necessary as the study aimed also to use real-time rain-gauge-adjusted radar data (RADOLAN) with 5 min resolution. Such data are not yet provided by the Deutscher Wetterdienst. The input data for the factors *L*, *S*, *K* and *P* were taken from the erosion database of the Bavarian administration. Information on crop and cultivation management was taken from a field-specific inventory. Appropriate values for c_{SLR} were used from literature.

The general validity of the USLE was tested by regression analyses of visual soil loss class versus estimated soil loss of all 8100 fields. Additionally, the validity of each individual USLE factor was tested using regression analysis and Pearsons' correlation coefficient *r*. For this,

the total validation data set was subdivided into 6 to 20 subsets according to the value range of an individual factor. This procedure was repeated for each of the six factors resulting into 88 subsets of average visually classified soil loss versus average estimated soil loss. The common relation including all 88 subsets was used as reference to test with scatter plots whether the subsets of any factor showed directional deviation from the common relation.

3 Abstracts of manuscripts and contributions of the authors

Three manuscripts resulted from this project and compose this thesis. In the following, the publication status, the abstracts and the contributions of the authors are presented.

3.1 Manuscript 1: Temporal- and spatial-scale and positional effects on rain erosivity derived from point-scale and contiguous rain data

Franziska K. Fischer, Tanja Winterrath, Karl Auerswald

Published in Hydrology and Earth System Sciences, 22, 6505-6518, 2018. DOI: 10.5194/hess-22-6505-2018

Up until now, erosivity required for soil loss predictions has been mainly estimated from rain gauge data at point scale and then spatially interpolated to erosivity maps. Contiguous rain data from weather radar measurements, satellites, cellular communication networks and other sources are now available, but they differ in measurement method and temporal and spatial scale from data at point scale. We determined how the intensity threshold of erosive rains has to be modified and which scaling factors have to be applied to account for the differences in method and scales. Furthermore, a positional effect quantifies heterogeneity of erosivity within 1 km², which presently is the highest resolution of freely available gauge-adjusted radar rain data. These effects were analysed using several large data sets with a total of approximately 2 x 10^6 erosive events (e.g. records of 115 rain gauges for 16 years distributed across Germany and radar rain data for the same locations and events). With decreasing temporal resolution, peak intensities decreased and the intensity threshold was met less often. This became especially pronounced when time increments became larger than 30 min. With decreasing spatial resolution, intensity peaks were also reduced because additionally large areas without erosive rain were included within one pixel. This was due to the steep spatial gradients in erosivity. Erosivity of single events could be zero or more than twice the mean annual sum within a distance of less than 1 km. We conclude that the resulting large positional effect requires use of contiguous rain data, even over distances of less than 1 km, but at the same time contiguously measured radar data cannot be resolved

to point scale. The temporal scale is easier to consider, but with time increments larger than 30 min the loss of information increases considerably. We provide functions to account for temporal scale (from 1 min to 120 min) and spatial scale (from rain gauge to pixels of 18 km width) that can be applied to rain gauge data of low temporal resolution and to contiguous rain data.

Franziska Fischer and Karl Auerswald designed the analysis, which was mainly carried out by Franziska Fischer. Tanja Winterrath provided most data and the knowledge about all steps involved in radar data creation. Franziska Fischer and Karl Auerswald prepared the manuscript with contributions by Tanja Winterrath.

3.2 Manuscript 2: Spatio-temporal variability of erosivity estimated from highly resolved and adjusted radar rain data (RADOLAN)

Franziska Fischer, Julia Hauck, Robert Brandhuber, Elmar Weigl, Harald Maier, Karl Auerswald

Published in Agricultural and Forest Meteorology, 223, 72-80, 2016. DOI: 10.1016/j.agrformet.2016.03.024

Rainfall events exhibit high spatio-temporal variability and cause soil erosion when thresholds of rainfall amount or intensity are exceeded. Analogously high variability in space and time is assumed for erosivity (*R*). RADOLAN, from the German Weather Service, provides radar rainfall data at high spatio-temporal resolution (1 × 1 km^2, 5 min), adjusted in 60 min intervals by measurements from a dense rain-gauge network that potentially could overcome present limitations of former *R* estimations from sparse rain gauges. The new database was used to analyse the spatio-temporal variability of rain depth and *R* for single events (event *R*) which occurred in an area of ~15 000 km^2 in southern Germany over a period of two years to illustrate the need for such high spatio-temporal resolution in rain data for *R* estimations. Further, the effect of calibrating 5 min resolved radar data using hourly

adjustment factors to rain-gauge data was explored. The spatial gradients of event *R* were steep, even steeper than for rain intensity, and call for such highly resolved data. Erosivity exhibited a clear maximum late in the afternoon. Daily rainfall differed from erosive rainfall due to rain breaks and rain extending over more than one day. Event *R* between adjacent 1 km^2 cells differed by up to 120 N h^{-1}. Even on an annual scale, erosivity at grid cells not further than 10 km apart could differ by more than a factor of five. Adjustment of the rain data was indispensable when calculating event *R* because adjustment could change event *R* by a factor of two. Even if long-term averages are used, differences by lacking adjustment would not be levelled. RADOLAN thus provides, for the first time, rain data as required in distributed erosion modelling for time periods shorter than 20 years.

Franziska Fischer and Karl Auerswald designed the analysis, which was mainly carried out by Franziska Fischer with contributions by Julia Hauck. Elmar Weigl, Harald Maier and Robert Brandhuber provided the data. Franziska Fischer drafted the manuscript which was revised by Karl Auerswald and reviewed by all other co-authors.

3.3 Manuscript 3: Validation of official erosion modelling based on high-resolution radar rain data by aerial photo erosion classification

Franziska Katharina Fischer, Michael Kistler, Robert Brandhuber, Harald Maier, Melanie Treisch, Karl Auerswald

Published in Earth Surface Processes and Landforms, 43, 187-194, 2018. DOI: 10.1002/esp.4216

The universal soil loss equation (USLE) is the most frequently applied erosion prediction model and it is also implemented as an official decision-making instrument for agricultural regulations. The USLE itself has been already validated using different approaches. Additional errors, however, arise from input data and interpolation procedures that become necessary for field-specific predictions on a national scale for administrative purposes. In this

study, predicted event soil loss using the official prediction system in Bavaria (Germany) was validated by comparison with aerial photo erosion classifications of 8100 fields. Values for the USLE factors were mainly taken from the official Bavarian high-resolution (5 × 5 m^2) erosion cadastre. As series of erosion events were examined, the cover and management factor was replaced by the soil loss ratio. The event erosivity factor was calculated from high-resolution (1 × 1 km^2, 5 min), indirectly rain gauge-adjusted radar rain data (RADOLAN). Aerial photo erosion interpretation worked sufficiently well and average erosion predictions and visual classifications correlated closely. This was also true for data broken down to individual factors and different crops. There was no reason to assume a general invalidity of the USLE and the official parametrization procedures. Event predictions mainly suffered from errors in the assumed crop stage period and tillage practices, which do not reflect interannual and farm-specific variation. In addition, the resolution of radar data (1 km^2) did not seem to be sufficient to predict short-term erosion on individual fields given the strong spatial gradients within individual rains. The quality of the input data clearly determined prediction quality. Differences between USLE predictions and observations are most likely caused by parametrization weaknesses but not by a failure of the model itself.

Robert Brandhuber, Harald Maier and Karl Auerswald developed the concept of the study. All authors, in particular Michael Kistler, contributed to the acquisition of the data. Karl Auerswald and Franziska Fischer designed the analysis, which was mainly carried out by Franziska Fischer. The scientific background for data interpretation was mainly provided by Karl Auerswald. Franziska Fischer drafted the manuscript. Karl Auerswald revised the manuscript.

4 Main findings

Manuscript I: The use of weather radar data implies a change in temporal and spatial scale in addition to the methodological differences to rain-gauge measurements. This has profound influence on recorded rain intensity and in turn on the calculated R factor. To compensate for these changes in scales several corrections become necessary.

The I_{max30} threshold for erosive events was lowered with decreasing temporal resolution to keep the number of erosive events independent of temporal scale. This threshold correction was identical at point and at 1 x 1 km^2 scale. Additionally, a temporal scaling factor for *R* was required, which depended on the spatial scale of rain data. The increase of the temporal scaling factor with decreasing temporal resolution was steeper at point than at 1 x 1 km^2 scale for intervals longer 30 min while the increase was equal for intervals shorter 30 min.

The spatial scaling factors for *R* increased with decreasing spatial resolution. The scaling factor for erosivity derived from 1 x 1 km^2 radar rain data was 1.48 (95% confidence interval: 1.43 - 1.52). For erosivity derived from 1 x 1 km^2 spatially integrated rain-gauge data the scaling factor was 1.15 (95% confidence interval: 1.04 - 1.26). The difference in both scaling factors for same spatial resolution was caused by the peculiarities to measure rain by rain gauges and by radars. Erosivity analyses of the spatially integrated rain-gauge data also showed that even at 0.5 km x 0.5 km scale the spatial scaling factor was still 1.08 (95% confidence interval: 1.00 - 1.16).

While the scaling factors are suitable to scale long-term average annual erosivities, they are inadequate for individual events. The positional effects on event erosivity R_e, accounting for the effects of spatial scale, rain measuring method and event rain variability within 1 x 1 km^2 was considerable in both directions (R_e at point scale higher/lower than at 1 x 1 km^2 scale) and exceeded a factor of 2 in many cases. In 43% of all analysed event cases, the rain event was recorded as erosive only either at point or at 1 x 1 km^2 scale, because none of the erosivity thresholds was met at the other spatial scale respectively.

Manuscript II: The contiguous rain data from radar measurements enabled to analyse the spatial gradients of erosivity across total individual rain cells. Within the study area erosive events with a minimum extent of 1 km^2 (according to radar pixel size) occurred on 170 days in two years (2011, 2012). Consequently, almost every fourth day an erosive event happened. However, the mean annual number of days with the occurrence of an erosive event per 1 x 1 km^2 pixel was only 19.5 d. This already indicated a pronounced spatial variability and a small extent of erosive rain cells. The mean diameter of erosivity cells was about 27% shorter (9.7 km) than the diameter of rain cells (13.2 km). The mean gradient of R_e was 0.6 N h^{-1} km^{-1} and 13.3% km^{-1} when related to average R_e. This gradient was almost four times steeper than the mean gradient of corresponding rain depth (0.43 mm d^{-1} km^{-1} and 3.5% km^{-1}). On short distances (1.4 km) the mean gradients of R_e and of rain depth were even steeper (22% km^{-1} for R_e and 6% km^{-1} for rain depth). The gradients became also steeper for annual erosivities R_y (1.4 N h^{-1} km^{-1} in 2011 and 1.8 N h^{-1} km^{-1} in 2012) due to the partial overlap of subsequent erosive rains. The gradient remained almost the same for the biennial average of R_y (1.2 N h^{-1} a^{-1} km^{-1}) because even then the erosive rain cells did not amalgamate into a coherent pattern.

The erosive rains followed a pronounced diurnal cycle. Maximum rain intensities and the occurrence probability of I_{max30} showed a diurnal pattern with a pronounced peak late in the afternoon.

About 36% of the events did not start and end on the same day. Dry spells of at least 6 h separating two independent events were most probable in the morning hours. These dry spells occurred at 24% of all days with erosive events.

Manuscript III: RADOLAN radar rain data were used to calculate event erosivity for USLE soil loss estimations of individual erosive events. These soil loss estimates were validated by classifications of visible erosion damages at documented fields from aerial photos. The reliability of visual erosion classifications was confirmed by significant correlations (r^2 = 0.74 - 0.78, $p < 0.001$) and high Nash-Sutcliffe efficiencies (NSE = 0.70 - 0.76) of repeated,

independent classification runs. Mean calculated soil loss per visual soil loss class increased significantly with increasing visible erosion damages ($r^2 = 0.91$, $p < 0.001$, $n = 7$) but variability of calculated soil loss in each visual soil loss class was large (standard deviations between 7 and 46 t ha^{-1}).

Separating the 8100 fields documented on the aerial photographs into 88 subsets by a relatively narrow range of each USLE factor resulted in a significant relation of calculated and classified soil loss with $r^2 = 0.93$. From that common relation no relation of calculated and classified soil loss directionally deviated when the 88 subsets were restricted to those of each USLE factor, respectively. The subsets of the factors *K* and *R* caused a less scatter in average calculated and visually classified soil loss than the subsets of the factors *S*, *L*, *C*, and *P*. This was because latter factors were correlated and thus lead to a large combined effect. In contrast, factor *K* varied little between the different sites and rain erosivity was independent of land use and field topography and the spatial resolution of erosivity was lower than field scale.

5 Discussion

Since the adaptation of the USLE to German conditions by Schwertmann and co-workers, the USLE has become an important tool in erosion quantification, landscape planning and agricultural counselling (e.g. DIN, 2017; Feldwisch, 2011; LfL, 2017; LfULG, 2016). Most of the factors of the USLE have been refined and modified to consider new developments. Surprisingly, two deficits remained. First, an overall evaluation of the accuracy of soil loss predictions was missing. Second, the R factor remained identical especially in Bavaria since the early work of Rogler & Schwertmann (1981). The deficit of updated R factors existed although computing power and, by the establishment of weather radars, data availability has increased enormously since then. Additionally, a change of the R factor has likely happened due to the ongoing climate change (Burt et al. 2016, Fiener et al. 2013; Mueller & Pfister, 2011). This thesis aimed at working towards remedying both deficits.

5.1 Avail and constraints of radar-derived erosivity

When using weather radar data for R factor calculations it must be considered that the method of measuring rain and the temporal and spatial scale differs from that of rain-gauge data. The effect of these differences on erosivity estimated from radar data had not been treated previously. A temporal scale effect had already been noticed for rain-gauge data due to the differences in available data (Yin et al., 2007; Panagos et al., 2015) but this assessment was not unequivocal (Auerswald et al., 2015). The spatial scale effect for erosivity had not been studied due to the novelty of operational radar measurements in erosion research and the lack of long-term radar data sets required for R factor estimations. For example, Zhu et al. (2018) recognized an underestimation of radar-derived event erosivity in comparison to rain-gauge-derived erosivity but only data of 12 rain gauges and two years were used. Therefore, they could not explain the discrepancy between radar- and rain-gauge-derived erosivity by a spatial scale and method effect. While erosivity is expected to be underestimated by grid measurements of rain, there is an inverse concept in catchment

hydrology resulting to the so-called areal reduction factors. Depending on the duration and the return period of a rain event, these factors usually reduce rain intensity from rain-gauge measurements when scaled from point scale to catchment areas (Allen & DeGaetano, 2005; De Michele et al., 2001; Stewart, 1989). This conceptual difference arises from different intended purposes of spatial rain data. For issues in catchment hydrology, the average and the relative distribution of rain depth within a watershed is of interest (Asquith & Famiglietti, 2000). In contrast, for erosion analysis, the maximum rain intensity at point and field-scale is important because there erosion already occurs. The results of this thesis showed that average annual erosivity is underestimated when derived from (radar) rain data of spatial resolutions lower than point scale and temporal resolutions lower than 1 min (Manuscript I) and that the measuring method of rain by radar itself additionally causes an underestimation of erosivity. Therefore, this work developed scaling factors for erosivity which compensate for the underestimation caused by the temporal and spatial scale effects and the rain measurement method effect. The application of these scaling factors and of adjusted minimum thresholds for I_{max30} in case of temporal scaling proved to be imperative for R factor calculations. Until now, the scale and method effects on erosivity were not yet considered by others who calculated erosivities from radar rain data (e.g. Risal et al., 2018; Zhu et al., 2018). Importantly, the present scaling factors are only adequate for adjustments of long-term average annual erosivities as all three effects can vary strongly from event to event. However, this is of no concern for soil loss predictions in landscape planning and agricultural counselling, as such efforts are usually based on the expected long-term mean erosivity (e.g. Prasuhn et al., 2013; Treisch & Brandhuber, 2012; Van Rompaey et al., 2001). This is because they have to anticipate future average conditions while erosivity strongly varies from year to year (e. g. Fiener et al., 2013; Verstraeten et al., 2006a). The use of radar rain data together with the scaling factors developed in this thesis was a major step forward and enabled the establishment of a topical erosivity map for Germany (Fischer et al., 2018).

Despite the development of appropriate scaling factors to adjust long-term mean annual erosivity, large uncertainty still exists within a radar pixel for individual events due to the

pronounced heterogeneity of rain erosivity even on distances shorter than 1 km as shown by the positional effect in Manuscript I. The positional effect showed up again in the deep spatial gradients of event erosivity (Manuscript II) and was also evident from analysing aerial photographs (Manuscript III). The positional effect was responsible for fields exhibiting quite contrasting erosion marks within the same radar pixel despite these fields showed very similar soil and land use conditions. This within-pixel heterogeneity limits the use of weather radar data for the quantification of event soil loss. Presently, no alternative is operationally available, although there is a promising development for the enhancement of spatial contiguous rain data by the implementation of rain data derived from commercial microwave links (Chwala et al., 2016; Chwala et al., 2018; Goldshtein et al., 2009; Overeem et al., 2018) or by using information of windscreen wiper frequency of motorcars which is related to rain rate (Haberlandt & Sester, 2010). This requires a development of computing capacities to handle the strongly increasing amount of data with increasing data networking and data resolution. Nevertheless, it is not expected that the positional effect on event erosivity can be entirely eliminated by future measurement and processing developments. The analysis of the dense rain-gauge network in Manuscript I also showed pronounced rainfall variability for areas of 0.25 km². So, positional effects would still exist when the resolution of radar rain data products is increased to 0.5 km x 0.5 km. For that resolution Pedersen et al. (2010) determined a coefficient of variation for total event rain depth between 1% and 26%, and 10% on average of the analysed events. This variation would again be more pronounced for erosivity. Consequently, the exclusive use of rain-gauge data for event soil loss estimations seems to be unsuitable because an unreasonably high rain-gauge density would be required to capture the heterogeneity of events. The point measurements can hardly be applied over distances longer than 100 m due to the strong spatial rainfall variability. Also Einfalt & Scheibel (2015) found strong spatial variability of rain for heavy rain events and deviations between rain-gauge and radar measurements in Germany. All in all, it seems that the presently best rain database for erosion event analyses is rain-gauge-adjusted radar rain data. Therefore, the positional effects determined in this thesis can be expected to be of

importance for the interpretation of individual soil loss events in the future. Poesen (2017) claimed further analysis to understand the complex processes of soil erosion. The strong variability of erosivity triggers the complexity of erosion processes and therefore, the finding of the positional effects might contribute to understand these processes. The positional effect should seriously be considered in erosion studies.

Regarding the analysis of individual erosive events, it is highly recommended to use 5 min instead of 60 min radar data to keep the degree of smoothing as low as possible. Five min is the highest temporal resolution of radar rain data (e.g. RY-RADOLAN) which is presently available from the Deutscher Wetterdienst (DWD, 2018a). Currently, those 5 min real-time data cannot be adjusted by rain-gauge data directly but indirectly by rain-gauge-adjusted 60 min RW-RADOLAN data when required immediately after the event (as described in Chapter 2.2.1 for YW-RADKLIM). For events further back in the past, the product YW-RADKLIM became recently (2018) available by the Deutscher Wetterdienst (Winterrath et al., 2018b). YW-RADKLIM data are 5 min radar data (RY-RADKLIM) indirectly adjusted by rain-gauge-adjusted and revised 60 min RW-RADKLIM data (see Chapter 2.2.1). Additionally, it is also recommended to use continuous data series of consecutive days to cover the complete duration of erosive events especially for event analyses. This is because events frequently do not start and end on the same day (Manuscript II). Although there is a clear diurnal pattern in the occurrence of erosive events (Manuscript II) which is in accordance to rain maxima (Paulat et al., 2008; Twardosz, 2007) and a peak of lightening activity in the late afternoon (Finke & Hauf, 1996), errors in erosivity estimates can arise when data are split at any time.

So far, studies about the spatial pattern of erosivity were restricted to point rain data recorded by rain gauges (e.g. Fiener & Auerswald, 2009; Hastings et al., 2005; Renard & Simanton, 1975). The usage of contiguously measured radar rain data in this work enabled to determine the total extent of (erosive) rain cells, independent of their spatial occurrence within the radar coverage, and to determine their spatial variability in rain intensity and

erosivity. The second study of this thesis showed considerably stronger gradients and smaller cells for erosivity than for rain depth of individual rain events (Manuscript II). The variability of erosivity in individual events and of their spatial occurrence in the study area of ~15 000 km² also resulted in strong gradients of annual erosivities and of biennial averages of annual erosivity. The dominance of individual erosive events within the spatial pattern of annual erosivity is not expected to disappear within a period of three, four or five years. This arises from the limited spatial extent of erosive events, their strong gradients and their high inter- and intra-annual variability. Even for a data set covering 17 years and 452 503 km² of Germany, the scatter of average annual erosivity was pronounced (Fischer et al., 2018). Multiple smoothing steps were necessary to level out this spatio-temporal variability and to extract spatial and temporal patterns. A meta-analysis showed that most erosion experiments under natural rain conditions last no longer than five years (Gracía-Ruiz et al., 2015). During such a short period, positional effects will not level out. Several rain gauges, or other methods to resolve the spatial gradient of rain within the area covered by such experiments, would hence be helpful to reduce unexplained variation.

5.2 Validity of RADOLAN-based soil loss predictions with the USLE

A data set of about 10 000 plot-years was necessary to develop the USLE as a robust soil loss prediction model which copes with the large natural variability and the high number of factor combinations influencing soil erosion. From time to time the data set was even expanded for revisions of the USLE (for an overview see Renard et al., 2011 and Laflen & Flanagan, 2013). For the validation of the USLE in this thesis, observations over two years and 8100 fields distributed over a large, diverse area (Bavaria, Germany) were used. This covered a large variety of agricultural site and cultivation conditions. Such a large variety of conditions as captured by the large area used in Manuscript III had not been covered before at field scale or by any other validation approach, like either by watershed studies or by tracer or by mapping studies. The validation in Manuscript III showed that the USLE, as it is

applied institutionally, is suitable for calculations of average soil loss. Calculated soil loss increased significantly with increasing erosion damages of the fields as they were visible in the aerial photos. This result suggests that the USLE is also valid for predictions of long-term average annual soil loss.

Nevertheless, there was a strong variability of calculated soil loss per class of visible erosion damages. This strong variability was mainly caused by two limiting factors, namely assumptions of the crop stage, and thereby of the soil loss ratio, and the positional effect of rain erosivity.

Soil loss ratios are usually determined according to crop stage periods and typical dates for these periods are assumed (see Schwertmann et al., 1990). This approach was also followed in the validation study because the aim was to validate the USLE as it is applied institutionally and used for agricultural counselling based on long-term averages. It does not account for inter- and intra-annual variability of growing periods and the individual farmer behaviour. Both factors can cause deviations between expected long-term average and recent cultivation and plant development status on the fields. Furthermore, the crop stage periods might also have changed due to a general change in plant development and farmer behaviour since their establishment in the 1980s (Schwertmann et al., 1990). Some studies already showed an earlier beginning of plant development in spring and a change in cultivation activities by the farmers (Chmielewski et al., 2004; Menzel et al., 2006). A number of approaches already exist to update crop stage periods, e.g. by the determination of soil cover using satellite imagery (Möller et al., 2017), or airborne hyperspectral HyMap data (Malec et al., 2015), or by kriging-based interpolation of phenological observations (Gerstmann et al., 2016). Those approaches could also be used for an update of C factors in Germany. This is additionally required as also the seasonal distribution of erosivity, which is included in C factor calculations, has changed towards an increased percentage of annual erosivity in winter months (Fischer et al., 2018).

The second main factor causing strong variability of predicted soil loss per class of visible erosion damages was identified to be the positional effect as discussed in the previous chapter. However, the positional effects are not adversely affecting the validity of the USLE as they are expected to level out in the long term (>> 10 years) and thus do not bias long-term soil loss predictions.

5.3 Avail of aerial photos in erosion research

For erosion events of particular importance, it may be a practical approach of reasonable effort to combine soil loss estimates of events with visual observations of soil loss damages by aerial photos. This approach was already successfully followed for several heavy rainstorms causing exceptional erosion and runoff damages in 2016 (Brandhuber et al., 2017; Hänsel et al., 2018). In Brandhuber et al. (2017) RADOLAN data were used to determine the severity of rainfalls and the pattern of the rain cells and their erosivity. The local general erosion susceptibility was identified by USLE long-term average soil loss predictions taken from appropriate official maps (comparable to the one in Treisch & Brandhuber, 2012). For those sites that combined high erosivity with high erosion susceptibility, aerial photos could be ordered. Evaluations of these aerial photos combined with a few on-site observations showed that sediment delivery did not only arise from sheet and (inter-)rill erosion of agricultural fields but also partly from ephemeral gully erosion (Brandhuber et al., 2017). Ephemeral gully erosion is caused by concentrated runoff (Poesen et al., 1996) and is not considered by the USLE (Wischmeier and Smith, 1978). Therefore, the total extent of erosion damages by this event could not have been estimated by USLE soil loss estimates exclusively but requires specific models like the Ephemeral Gully Erosion Model EGEM (Woodward, 1999; Nachtergaele et al., 2001) or the Ephemeral Gully Erosion Estimator EphGEE that can be added to the (R)USLE (Dabney et al., 2014; Vieira et al., 2014). A different approach for the reconstruction of an exceptional erosion event in 2016

was followed by Hänsel et al. (2018) by using the model Erosion3D and radar rain data for event soil loss estimations.

Aerial photos may additionally help to find adequate erosion control measures for individual sites. Flow paths of concentrated runoff can be identified by aerial photos (Manuscript III; see Fig. 4). Along those flow paths grassed waterways can be installed to reduce erosion and to have additional positive effects such as sediment retention (e.g. Atkins & Coyle, 1977; Fiener & Auerswald, 2003). Such measures should additionally be combined with on-site erosion control measures such as, e.g., strip mulch tillage, reduced tillage, no-tillage and cover crops. For a descriptive example of sustainable soil use at landscape scale see Auerswald et al. (2000). The efficiency of installed erosion control measures could then again be evaluated by aerial photos taken after erosive rain events. RADOLAN provides a convenient tool to identify strong erosive rains and enables to immediately order aerial photographs when signs of erosion are still fully visible.

The widespread application of effective erosion control is also of great importance to reach the objectives of the European Water Framework Directive (EU, 2000) due to the off-site effects of soil erosion. A widely applied measure in Europe is the setup of riparian vegetated filter strips which can also be subsidized (EU, 2013; BMEL, 2015). However, the efficiency of these strips for sediment control is questionable at landscape scale (Verstraeten et al., 2006b). Therefore, combinations of different erosion control measures are indispensable to achieve most effective erosion control. For an efficiency assessment of different soil conservation measures see for example Maetens et al. (2012). Nevertheless, the principles of soil conservation techniques are known since several decades (Bennett, 1939; Bennett, 1947) and a large number of studies on erosion control measures has already been carried out (e.g. a Google Scholar search with the keywords '"soil erosion" "control measure"' returned about 28 400 hits). Surprisingly, erosion control measures seem not to be implemented sufficiently (e.g. Auerswald et al., 2018; Posthumus et al., 2011). It was shown based on the data set of Manuscript III that even relatively simple erosion control measures

are rarely or not consequently applied (Auerswald et al., 2018). Unawareness of the positive effects of measures to prevent erosion and the fear of financial losses are frequently named for non-adopting of erosion control measures by farmers according to evaluated questionnaires (e.g. Bijttebier et al., 2015; Yeboah et al., 2015). In general, the non-adopting might also be encouraged by the general public ignorance of soil erosion as threat which needs urgent prevention (García-Ruiz et al., 2017).

However, the consequent implementation of erosion control measures is indeed now of increased urgency. By climate change the number of erosion-relevant rains (Mueller & Pfister, 2011) and rain erosivity has already increased since the last decades (Fiener et al., 2013). An increase in erosivity of around 66% over four decades was also shown by the comparison of the past German R factor map from Sauerborn (1994) and the new German R factor map (Fischer et al., 2018). An ongoing and even stronger increase in rain intensity (Berg et al., 2013) and thus in rain erosivity and also in soil loss (Routschek et al., 2014) is expected by global warming. The increase of erosion then may come along with an increase of on-site and off-site damages by erosion which again may also increasingly endanger food security and the quality of aquatic systems (Pimentel, 2006) and human properties (Bachmair & Faust, 2017). This scenario calls for an urgent practical implementation of the knowledge gained from scientific studies about erosion and control measures.

6 Conclusions

The results of this thesis suggest that long-term average soil loss can be estimated reliably by the Bavarian institutional version of the USLE. The R factor derived from RADOLAN / RADKLIM radar rain data from the Deutscher Wetterdienst requires scaling factors depending on the spatial and temporal resolution of the radar product. These scaling factors enabled an update of the German R factor map by RADKLIM data set covering 17 years. This is a major step forward given that the R factor of several federal states had not been updated since almost 40 years despite an on-going climate change, and given that the R factors were based on relatively short data series of sparsely distributed rain gauges. Now, it is of high urgency to use soil loss predictions based on the new R factors for a consequent implementation of erosion control measures where necessary.

Acknowledgements

This thesis is the result of an outstanding support by several persons of the three cooperating institutions Bayerische Landesanstalt für Landwirtschaft (LfL), Technische Universität München (TUM) and Deutscher Wetterdienst (DWD) and additionally of the Leibniz Rechenzentrum (LRZ). The thesis is based on the project 'Ermittlung des Raum- und Jahreszeitmusters der Regenerosivität in Bayern aus radargestützten Niederschlagsdaten zur Verbesserung der Erosionsprognose mit der Allgemeinen Bodenabtragsgleichung' which was funded by the Bayerisches Staatsministerium für Ernährung, Landwirtschaft und Forsten (A/15/17) and initialized by Karl Auerswald (TUM), Robert Brandhuber (LfL) and Harald Maier (DWD). All three persons enabled me to carry out this project successfully as they gave me support wherever and whenever necessary.

I would like to express my sincere gratitude to my supervisor Karl Auerswald who made enormous effort to teach me critical thinking, scientific analysing, writing and presenting. I would like to express my sincere gratitude to Robert Brandhuber for enabling me to concentrate on working on the project and for his confidence in my work. I would like to express my sincere gratitude to Harald Maier for all his efforts to provide me access to all necessary data of the Deutscher Wetterdienst. Moreover I would like to thank all three project leaders for sharing their working and life experiences with me.

Sincere gratitude goes to my mentor Tanja Winterrath for her important specialist and mental support. She contributed significantly to the success of this project.

Nevertheless, it would not have been possible to carry out this project without the support of many other staff members of the four institutions LfL, TUM, DWD and LRZ. I would like to thank Melanie Treisch and Michael Kistler (LfL) for answering a countless number of specialist and bureaucratic questions and also for our friendly relationship. I would like to thank Peter Wanzek (DWD, Weihenstephan), Mario Hafer, Christoph Brendl, Thomas Junghänel and Wolfgang Janssen (DWD, Offenbach a. M.) for their patient and helpful support and access to data. I would like to thank Christian Zang and Thomas Machl (TUM)

for their advices regarding processing and management of big data sets. I would like to thank the staff working for the service desk of the LRZ for their patient, helpful and quick support in the processing of data via the servers of the LRZ. I would like to thank Christoph Lehmeier for this fruitful input in the end of my PhD. I would also like to thank the staff of the Graduate Center Weihenstephan for their helpful support.

Last but not least, I would like to thank all members of the Grassland group, especially Prof. Schnyder, for the hospitable, helpful and warm atmosphere. I enjoyed the time at the chair a lot.

Beside all persons who have been working together with me, I would like to express my sincere gratitude to all my friends and my family for always being so considerate, lenient and optimistic.

References

Allen, R.J., DeGaetano, A.T., 2005. Areal reduction factors for two eastern United States regions with high rain-gauge density. Journal of Hydrologic Engineering, 10, 327-335. DOI: 10.1061/~ASCE!1084-0699~2005!10:4~327!.

Aniol, R., 1975. Flächenausdehnung kurzer Starkregen in einem dichten Regenschreibernetz. Tagungsbericht Interpraevent, 149-158.

Arnold, J.G., Srinivasan, R., Muttiah, R.S., Williams, J.R., 1998. Large area hydrologic modelling and assessment: Part I. Model development. Journal of the American Water Resources Association, 34, 73-89.

Asquith, W.H., Famiglietti, J.S., 2000. Precipitation areal-reduction factor estimation using an annual-maxima centered approach. Journal of Hydrology, 230, 55-69. DOI: 10.1016/S0022-1694(00)00170-0.

Atkins, D.M., Coyle, J.J., 1977. Grass waterways in soil conservation. USDA Leaflet 477. U.S. Gov. Print. Office, Washington, DC.

Auerswald, K., 1986a. Einstufung der Bodenerodibilität (K-Faktor) nach dem Klassenbeschrieb der Reichsbodenschätzung für Südbayern. Zeitschrift für Kulturtechnik und Flurbereinigung, 27, 344-351.

Auerswald, K., 1986b. Eignung der Hangneingungsfaktoren verschiedener Erosionsmodelle unter bayerischen Anbauverhältnissen. Zeitschrift für Kulturtechnik und Flurbereinigung, 27, 218-224.

Auerswald, K., 1991. Onsite- und Offsite-Schäden durch Bodenerosion. Berichte über Landwirtschaft, Sonderheft, 205, 75-82.

Auerswald, K., 1992. Verfeinerte Bewertung von Erosionsschutzmaßnahmen unter deutschen Anbaubedingungen mit dem P-Faktor der Allgemeinen

Bodenabtragsgleichung (ABAG). Zeitschrift für Kulturtechnik und Landentwicklung, 33, 137-144.

Auerswald, K., 2002. Schätzung des C-Faktors aus Fruchtartenstatistiken für Ackerflächen in Gebieten mit subkontinentalem bis subatlantischem Klima nördlich der Alpen [Estimating the C Factor of the Universal Soil Loss Equation from Cropping Statistics for Sites with Sub-Continental to Sub-Atlantic Climate North of the Alps]. Zeitschrift für Landnutzung und Landentwicklung, 43, 1-5.

Auerswald, K., Albrecht, H., Kainz, M., Pfadenhauer, J., 2000. Principles of sustainable land-use systems developed and evaluated by the Munich Research Alliance on agro-ecosystems (FAM). Petermanns Geographische Mitteilungen, 144, 16-25.

Auerswald, K., Elhaus, D., 2013. Ableitung der Bodenerodierbarkeit K anhand der Bodenart. Bodenschutz, 4, 109-113.

Auerswald, K., Elhaus, D., Martin, W., 2016b. Wassererodierbarkeit von Böden der Bodenart Sand (Ss). Bodenschutz, 2, 42-45.

Auerswald, K., Fiener, P., Gomez, J.A., Govers, G., Quinton J.N., Strauss, P., 2015. Comment on “Rainfall erosivity in Europe” by Panagos et al. (Sci. Total Environ., 511, 801–814, 2015), Science of the Total Environment, 532, 849-852. DOI: 10.1016/j.scitotenv.2015.05.019.

Auerswald, K., Fiener, P., Martin, W., Elhaus, D., 2014. Use and misuse of the K factor equation in soil erosion modeling: An alternative equation for determining USLE nomograph soil erodibility values. Catena, 118, 220-225. DOI: 10.1016/j.catena.2014.01.008.

Auerswald, K., Fiener, P., Martin, W., Elhaus, D., 2016a. Corrigendum to “Use and misuse of the K factor equation in soil erosion modeling“. Catena, 139, 271.

Auerswald, K., Fischer, F.K., Kistler, M., Treisch, M., Maier, H., Brandhuber, R., 2018. Behavior of farmers in regard to erosion by water as reflected by their farming practices. Science of the Total Environment, 613-614, 1-9. DOI: 10.1016/j.scitotenv.2017.09.003.

Auerswald, K., Flacke, W., Neufang, L., 1988. Räumlich differenzierende Berechnung großmaßstäblicher Erosionsprognosekarten – Modellgrundlagen der dABAG. Zeitschrift für Pflanzenernährung und Bodenkunde, 151, 369-373. DOI: 10.1002/jpln.19881510604. Online available at: https://onlinelibrary.wiley.com/doi/abs/10.1002/jpln.19881510604 (last access: 24 July 2018).

Auerswald, K., Kainz, M., 1998. Erosionsgefährdung (C-Faktor) durch Sonderkulturen. Bodenschutz, 3, 98-102.

Auerswald, K., Kainz, M., Vogl, W., 1986. Vergleich der Erosionsgefährdung durch Maisfruchtfolgen (C-Faktor). Bayerisches Landwirtschaftliches Jahrbuch, 63, 1-8.

Auerswald, K., Schwab, A., 1999. Erosionsgefährdung (C-Faktor) unterschiedlich bewirtschafteter Weinbauflächen. [Erosion risk (C factor) of different viticultural pratices]. Die Weinwissenschaft, 54, 54-60.

Auerswald, K., v. Perger P., 1998. Bodenerosion durch Wasser - Ursachen, Schutzmaßnahmen und Prognose mit PCABAG. AID-Heft, 1378, Publisher AID, Bonn.

Bachmair, S., Faust, E., 2017. Rainstorms over Europe. In: Topics Geo, Natural catastrophes 2016. Analyses, assessments, positions. 2017 issue. Munich Re Group, Munich. Online available at: https://www.munichre.com/topics-online/en/2017/topics-geo/rainstorms-over-europe#furtherinformation (last access: 20 April 2018).

Bakker, M.M., Govers, G., Jones, R.A., Rounsevell M.D.A., 2007. The effect of soil erosion on Europe's crop yields. Ecosystem, 10, 1209-1219. DOI: 10.1007/s10021-007-9090-3.

Bartels, H., Weigl, E., Reich, T., Lang, P., Wagner, A., Kohler, O., Gerlach, N., 2004. Projekt RADOLAN: Routineverfahren zur Online-Aneichung der Radarniederschlagsdaten mit Hilfe von automatischen Bodenniederschlagsstationen (Ombrometer). Deutscher Wetterdienst. Online available at: https://www.dwd.de/DE/leistungen/radolan/radolan_info/abschlussbericht_pdf.pdf?__blob=publicationFile&v=2 (last access: 13 November 2018).

Bennett, H.H., 1939. Soil conservation. New York and London: McGraw-Hill Book Company, Inc.. Online available at: https://babel.hathitrust.org/cgi/pt?id=mdp.39015067166226;view=1up;seq=339 (last access: 4 November 2018).

Bennett, H.H., 1947. Elements of soil conservation. New York: McGraw-Hill. Online available at: https://babel.hathitrust.org/cgi/pt?id=mdp.39015006862802;view=1up;seq=7 (last access: 4 November 2018)

Berg, P., Moseley, C., Haerter, J.O., 2013. Strong increase in convective precipitation in response to higher temperatures. Nature Geoscience 6, 181-185. DOI: 10.1038/NGEO1731.

Bijttebier, J., Ruysschaert, G., Hijbeek, R., Rijk, B., Werner, M., Raschke, I., Steinmann, H.H., Zylowska, K., Pronk, A., Schlatter, N., Guzmán, G., Syp, A., Bechini, L., Turpin, N., Guiffant, N., Perret, E., Mauhé, N., Toqué, C., Zavattaro, L., Costamagna, C., Grignani, C., Lehninen, T., Baumgarten, A., Spiegel, H., Portero, A., Van Walleghem, T., Pedrera, A., Laguna, A., Vanderlinden, K., Giráldez, V., 2015. Farmers review of best management practices: drivers and barriers as seen by adopters and non-adopters. Catch-C project. 7th Framework Programme for Research, Technological Development and Demonstration, Theme 2 – Biotechnologies, Agriculture & Food. Online available at: http://www.catch-c.eu/deliverables/D4.422_Farmers%20review%20of%20Best%20Management%20Pra

ctices%20-%20drivers%20and%20barriers%20as%20seen%20by%20adopters%20and%20non-adopters.pdf (last access: 4 November 2018).

BMEL – Bundesministerium für Ernährung und Landwirtschaft, 2015. Umsetzung der EU-Agrarreform in Deutschland. Online available at: https://www.bmel.de/SharedDocs/Downloads/Broschueren/UmsetzungGAPinD.pdf?__blob=publicationFile (last access: 5 November 2018).

Boardman, J., Poesen, J. (Eds.), 2006. Soil erosion in Europe. John Wiley & Sons, Chichester, 855 pp.

Boix-Fayos, C., Martínez-Mena, M., Arnau-Rosalén, E., Calvo-Cases, A., Castillo, V., Albaladejo, J., 2006. Measuring soil erosion by field plots: Understanding the sources of variation. Earth-Science Reviews, 78, 267-285. DOI: 10.1016/j.earscirev.2006.05.005.

Brandhuber, R., Treisch, M., Fischer, F., Kistler, M., Maier, H., Auerswald, K., 2017. Starkregen, Bodenabschwemmungen und Sturzfluten im Mai und Juni 2016: Landwirtschaft und Maisanbau. Schriftenreihe Bayerische Landesanstalt für Landwirtschaft, ISSN 1611-4159. Online available at: www.lfl.bayern.de/mam/cms07/publikationen/daten/schriftenreihe/starkregen-bodenerosion_sturzfluten_lfl-schriftenreihe.pdf (last access: 12 March 2018).

Burt, T., Boardman, J., Foster, I., Howden, N., 2016. More rain, less soil: Long-term changes in rainfall intensity with climate change. Earth Surface Processes and Landforms, 41, 563-566.

Carpenter, S.R., Caraco, N.F., Correll, D.L., Howarth, R.W., Sharpley, A.N., Smith, V.H., 1998. Nonpoint pollution of surface waters with phosphorus and nitrogen. Ecological Applications, 8, 559-568. DOI: 10.2307/2641247.

Castillo, C., Pérez, R., James, M.R., Quinton, J.N., Taguas, E.V., Gómez, J.A., 2012. Comparing the Accuracy of Several Field Methods for Measuring Gully Erosion. Soil Science Society of America Journal, 76, 1319-1332. DOI: 10.2136/sssaj2011.0390.

Chmielewski, F.-M., Müller, A., Bruns, E., 2004. Climate changes and trends in phenology of fruit trees and fields crops in German, 1961-2000. Agricultural and Forest Meteorology, 121, 69-78. DOI: 10.1016/S0168-1923(03)00161-8.

Chow, V.T., 1953. Frequency analysis of hydrologic data with special application to rainfall intensities. University of Illinois. Engineering Experiment Station. Bulletin 414. Online available at: www.ideals.illinois.edu/handle/2142/4107 (last access: 13 November 2018).

Chwala, C., Keis, F., Kunstmann, H., 2016. Real-time data acquisition of commercial microwave link networks for hydrometeorological applications. Atmospheric Measurement Techniques, 9, 991-999. DOI: 10.5194/amt-9-991-2016.

Chwala, C., Smiatek, G., Kunstmann, H., 2018. Real-time country-wide rainfall derived from a large network of commercial microwaves links in Germany. Geophysical Research Abstracts, 20, EGU2018-10096.

Cronshey, R.G., Theurer, F.D., 1998. AnnAGNPS: non-point pollutant loading model. In Proceedings of the First Federal Interagency Hydrologic Modeling Conference, Las Vegas, NV, 19–23 April; 9–16.

Dabney, S.M., Vieira, D.A.N, Yoder, D.C., 2014. Predicting ephemeral gully erosion with RUSLER and EphGEE. In: Sediment dynamics from the summit to the sea, edited by: Xu, J.Y, Allison, M.A., Bentley, S.J., Collins, A.L., Erskine, W.D., Golosov, V., Horowitz, A.J., Stone, M., IAHS Publication, 367, 72-79. DOI: 10.5194/piahs-367-72-2015.

De Michele, C., Kottegoda, N.T., Rosso, R., 2001. The derivation of areal reduction factor of storm rainfall from its scaling properties. Water Resources Research, 37, 3247-3252. DOI: 10.1029/2001WR000346.

De Vente, J., Poesen, J., 2005. Predicting soil erosion and sediment yield at the basin scale: scale issues and semi-quantitative models. Earth-Science Reviews, 71, 95-125. DOI: 10.1016/j.earscirev.2005.02.002.

DIN – Deutsches Institut für Normierung, 2017. DIN 19708: 2017-08 Bodenbeschaffenheit – Ermittlung der Erosionsgefährdung von Böden durch Wasser mit Hilfe der ABAG. Berlin, Germany.

DWD – Deutscher Wetterdienst, Hydrometeorologie, 2018a. Tabellarische Übersicht der RADOLAN-Produkte. Stand: 25.04.2018. Online available at: https://www.dwd.de/DE/leistungen/radolan/produktuebersicht/radolan_produktuebersicht_pdf.html (last access: 6 November 2018).

DWD – Deutscher Wetterdienst, Hydrometeorologie, 2018b. RADOLAN Kurzbeschreibung. Stand: April 2018. Online available at: https://www.dwd.de/DE/leistungen/radolan/radarniederschlagsprodukte/radolankurzbeschreibung_pdf.pdf?__blob=publicationFile&v=6 (last access: 19 December 2018).

Dymond, J.R., Hicks, D.L., 1986. Steepland erosion measured from historical aerial photographs. Journal of Soil and Water Conservation, 41, 252-255.

EU, European Parliament and the Council of the European Union, 2000. Directive 2000/60/EC establishing a framework for the Community action in the field of water policy. Official Journal of the European Communities, L327, 1-72. Online available at: https://eur-lex.europa.eu/resource.html?uri=cellar:5c835afb-2ec6-4577-bdf8-756d3d694eeb.0004.02/DOC_1&format=PDF (last access: 4 November 2018).

EU, European Parliament and the Council of the European Union, 2013. Regulation (EU) No 1307/2013 of the European Parliament and of the Council of 17 december 2013 establishing rules for direct payments to farmers under support schemes within the framework of the common agricultural policy and repealing Council Regulation (EC) No 637/2008 and Council Regulation (EC) No 73/2009. Official Journal of the European Communities, L347, 608-670. Online available at: https://eur-lex.europa.eu/legal-content/EN/TXT/?qid=1436267634754&uri=CELEX:32013R1307 (last access: 5 November 2018).

Einfalt, T., Scheibel, M., 2015. Vergleich von Extremwertstatistiken aus Radarmessungen und Regenschreibern. In: Evers, M., Diekkrüger, B., 2015. Aktuelle Herausforderungen im Flussgebiets-und Hochwassermanagement. Prozesse. Methoden. Konzepte. Beiträge zum Tag der Hydrologie am 19./20. März 2015 an der Universität Bonn. Forum für Hydrologie und Wasserbewirtschaftung, 35.15, pp 89-100. Online available at: www.fghw.de/download/forumsbeitraege/35.15_Gesamt.pdf (last access: 20 October 2018).

Ferro, V., Giordano, G., Iovino, M., 1991. Isoerosivity and erosion risk map for Sicily. Hydrological Sciences Journal, 36, 549-564. DOI: 10.1080/02626669109492543.

Feldwisch, 2011. Merkblatt - Gefahrenabwehr bei Bodenersoion. LUBW – Landesanstalt für Umwelt, Messungen und Naturschutz Baden-Württemberg. Online available at: https://www.lubw.baden-wuerttemberg.de/documents/10184/212002/merkblatt_gefahrenabwehr_bei_bodenerosion.pdf/38062e82-7fce-4f73-87ab-08b7b3d1c4a9 (last access: 3 November 2018).

Fiener, P, Auerswald, K., 2003. Effectiveness of grassed waterways in reducing runoff and sediment delivery from agricultural watersheds. Journal of Environmental Quality, 32, 927-936. DOI: 10.2134/jeq2003.0927.

Fiener, P., Auerswald, K., 2009. Spatial variability of rainfall on a sub-kilometre scale. Earth Surface Processes and Landforms, 34, 848-859. DOI: 10.1002/esp.1779.

Fiener, P., Neuhaus, P. Botschek, J., 2013. Long-term trends in rainfall erosivity – analysis of high resolution precipitation time series (1937 – 2007) from Western Germany. Agricultural and Forest Meteorology, 171-172, 115-123. DOI: 10.1016/j.agrformet.2012.11.011.

Finke, U., Hauf, T., 1996. The characteristics of lightening occurrence in southern Germany. Beiträge zur Physik der Atmosphäre, 69, 361-374.

Fischer, F.K., Winterrath, T., Auerswald, K., 2018. Rain erosivity map for Germany derived from contiguous radar rain data. Hydrology and Earth System Sciences Discussions, in review. DOI: 10.5194/hess-2018-504.

Flacke, W., Auerswald, K., Neufang, L., 1990. Combining a modified Universal Soil Loss Equation with a digital terrain model for computing high resolution maps of soil loss resulting from rain wash. Catena, 17, 383-397. DOI: 10.1016/0341-8162(90)90040-K.

Flügel, W.-A., Märker, M., Moretti, S., Rodolfi, G., Staudenrausch, H., 1999. Soil erosion hazard assessment in the Mkomazi river catchment (Kwa Zulu/Natal-South Africa) by using aerial photo interpretation. Zentralblatt fuer Geologie und Paläontologie, 1, 1-13.

Foster, G.R., 2005. Draft: Science Documentation. Revised Universal Soil Loss Equation version 2 (RUSLE2). USDA – Agricultural Research Service, Washington, DC. Online available at: www.ars.usda.gov/ARSUserFiles/64080530/RUSLE/RUSLE2_Science_Doc.pdf (last access: 13 November 2018).

Foster, G.R., Wischmeier, W.H., 1974. Evaluating irregular slopes for soil loss prediction. Transactions of the ASAE, 17, 305-309. DOI: 10.13031/2013.36846.

García-Ruiz, J.M., Beguería, S., Lana-Renault, N., Nadal-Romero, E., Cerdà, A., 2017. Ongoing and emerging questions in water erosion studies. Land Degradation and Development, 28, 5-21. DOI: 10.1002/ldr.2641.

García-Ruiz, J.M., Beguería, S., Nadal-Romero, E., González-Hidalgo, J.C., Lana-Renault, N., Sanjuán, Y., 2015. A meta-analysis of soil erosion rates across the world. Geomorphology, 239, 160-173. DOI: 10.1016/j.geomorph.2015.03.008.

Gerstmann, H., Doktor, D., Gläßer, C., Möller, M., 2016. PHASE: A geostatistical model for the Kriging-based spatial prediction of crop phenology using public phenological and climatological observations. Computers and Electronics in Agriculture, 127, 726-738. DOI: .10.1016/j.compag.2016.07.032.

González-Hidalgo, J.C., de Luis, M., Batalla, R.J., 2009. Effects of the largest daily events on total soil erosion by rainwater. An analysis of the USLE database. Earth Surface Processes and Landforms, 34, 2070-2077. DOI: 10.1002/esp.1892.

Goldshtein, O., Messer, H., Zinevich, A., 2009. Rain rate estimation using measurements from commercial telecommunications links. IEEE Transactions on Signal Processing, 57, 1616-1625. DOI: 10.1109/TSP.2009.2012554.

Grieve, I.C., Davidson, D.A., Gordon, J.E., 1995. Nature, extent and severity of soil erosion in upland Scotland. Land Degradation and Development, 6, 41-55. DOI: 10.1002/ldr.3400060105.

Haberlandt, U., Sester, M., 2010. Areal rainfall estimation using moving cars as rain gauges – a modelling study. Hydrology and Earth System Sciences, 14, 1139-1151. DOI: 10.5194/hess-14-1139-2010.

Habib, E., Krajewski, W. F., Kruger, A., 2001. Sampling errors of tipping-bucket rain gauge measurements. Journal of Hydrologic Engineering, 6, 159-166. DOI: 10.1061/(ASCE)1084-0699(2001)6:2(159).

Hastings, B.K., Breshears, D.D., Smith, F.M., 2005. Spatial variability in rainfall erosivity versus rainfall depth. Vadose Zone J., 4, 500-504. DOI: 10.2136/vzj2004.0036.

Helmert, K., Tracksdorf, P., Steinert, J., Werner, M., Frech, M., Rathmann, N., Hengstebeck, T., Mott, M., Schumann, S., Mammen, T., 2014. DWDs new radar network and post-processing algorithm chain. 8th European Conference on Radar in Meteorology and Hydrology (ERAD), Garmisch-Partenkirchen, Germany, September 2014. Online available at: http://www.pa.op.dlr.de/erad2014/programme/ExtendedAbstracts/237_Helmert.pdf (last access: 19 December 2018).

Istok, J.D., McCool, D., King, L.G., Boersma, L., 1986. Effect of rainfall measurement interval on EI calculation. Transactions of the ASAE, 29, 730-734. DOI: 10.13031/2013.30221.

Jacobi, S., Bronstert, A., Heistermann, M., 2014. Rain rate retrieval of partially blocked beams from single-polarized weather radar data. 8th European Conference on Radar in Meteorology and Hydrology (ERAD), Garmisch-Partenkirchen, Germany, September 2014. Online available at: http://www.pa.op.dlr.de/erad2014/programme/ExtendedAbstracts/128_Jacobi.pdf (last access: 19 December 2018).

Janeček, M., Květoň, V., Kubátová, E., Kobzová, D., Vošmerová, M., Chlupsová, J., 2013. Values of rainfall erosivity factor for the Czech Republic. Journal of Hydrology and Hydromechanics, 61, 97-102. DOI: 10.2478/johh-2013-0013.

Kagerer, J., Auerswald, K., 1997. Erosionsprognose-Karten im Maßstab 1:5000 für Flurbereinigungsverfahren und Landwirtschaftsberatung. Bayerische Landesanstalt für Bodenkultur und Pflanzenbau. Freising, Germany.

Krajewski, W.F., Ciach, G.J., Habib, E., 2003. An analysis of small-scale rainfall variability in different climatic regimes. Hydrological Sciences Journal, 48, 151-162. DOI: 10.1623/hysj.48.2.151.44694.

Laflen, J.M., Flanagan, D.C., 2013. The development of U. S. soil erosion prediction and modelling. International Soil and Water Conservation Research, 1, 1-11. DOI: 10.1016/S2095-6339(15)30034-4.

Laws, J.0., 1941. Measurement of fall velocity of water drops and rain drops. Transactions American Geophysical Union, 22, 709-721. DOI: 10.1029/TR022i003p00709.

Laws, J.0., Parsons, D.A., 1943. The relation of raindrop size to intensity. Transactions American Geophysical Union, 24, 452-459. DOI: 10.1029/TR024i002p00452.

LfL – Bayerische Landesanstalt für Landwirtschaft, 2017. Bodenerosion – Wie stark ist die Bodenerosion auf meinen Feldern? 7th Edition. Online available at: https://www.lfl.bayern.de/mam/cms07/publikationen/daten/informationen/bodenerosion_lfl-information.pdf (last access: 3 November 2018).

LfULG – Sächsisches Landesamt für Umwelt, Landwirtschaft und Geologie, 2016. Gefahrenabwehr bei Bodenerosion. Arbeitshilfe. 2nd Edition, 28 pp. Online available at: https://publikationen.sachsen.de/bdb/artikel/20533 (last access: 3 November 2018).

Lochbihler, K., Lenderink, G., Siebesma, A. P., 2017. The spatial extent of rainfall events and its relation to precipitation scaling, Geophysical Research Letters, 44, 8629-8636. DOI: 10.1002/2017GL074857.

Lufafa, A., Tenywa, M.M., Isabirye, M., Majaliwa, M.J.G., Woomer, P.L., 2003. Prediction of soil erosion in a Lake Victoria basin catchment using GIS-based Universal Soil Loss model. Agricultural Systems, 76, 883-894. DOI: 10.1016/S0308-521X(02)00012-4.

Maetens, W., Poesen, J., Vanmaercke, M., 2012. How effective are soil conservation techniques in reducing plot runoff and soil loss in Europe and the Mediterranean? Earth-Science Reviews, 115, 21-36. DOI: 10.1016/j.earscirev.2012.08.003.

Malec, S., Rogge, D., Heiden, U., Sanchez-Azofeifa, A., Bachmann, M., Wegmann, M., 2015. Capability of spaceborne hyperspectral EnMAP mission for mapping fractional

cover for soil erosion modeling. Remote Sensing, 7, 11776-11800. DOI: 10.3390/rs70911776.

Martin, W., 1988. Die Erodierbarkeit von Böden unter simulierten und natürlichen Regen und ihre Abhängigkeit von Bodeneigenschaften. Dissertation, TU München.

Menzel, A., von Vopelius, J., Estrella, N., Schleip, C., Dose, V., 2006. Farmers‘ annual activities are not tracking speed of climate change. Climate Research, 32, 201-2017. Online available at: https://www.int-res.com/abstracts/cr/v32/n3/p201-207/ (last access: 2 November 2018).

Möller, M., Gerstmann, H., Gao, F., Dahms, T.C., Förster, M., 2017. Coupling of phenological information and simulated vegetation index time series: Limitations and potentials for the assessment and monitoring of soil erosion risk. Catena, 150, 192-205. DOI: 10.1016/j.catena.2016.11.016.

Morgan, R.P.C., Quinton, J.N., Smith, R.E., Govers, G., Poesen, J., Auerswald, K., Chisci, G., Torri, D., Styczen, M.E., 1998. The European Soil Erosion Model (EUROSEM): a dynamic approach for predicting sediment transport from fields and small catchments. Earth Surface Processes and Landforms, 23, 527-544. DOI: 10.1002/(SICI)1096-9837(199806)23:6<527::AID-ESP868>3.0.CO;2-5.

Mueller, E.N., Pfister, A., 2011. Increasing occurrence of high-intensity rainstorm events relevant for the generation of soil erosion in a temperate lowland region in Central Europe. Journal of Hydrology, 411, 266-278. DOI: 10.1016/j.jhydrol.2011.10.005.

Nachtergaele, J., Poesen, J., Vandekerckhove, L., Oostwoud Wijdenes, D., Roxo, M., 2001. Testing the ephemeral gully erosion model (EGEM) for two Mediterranean environments. Earth Surface Processes and Landforms, 26, 17-30. DOI: 10.1002/1096-9837(200101)26:1<17::AID-ESP149>3.0.CO;2-7.

Nash, J.E., Sutcliffe, J.V., 1970. River flow forecasting through conceptual models. Part I. A discussion of principles. Journal of Hydrology 10, 282-290.

Nearing, M.A., Govers, G., Norton, D.L., 1999. Variability in soil erosion data from replicated plots. Soil Science Society of America Journal, 63, 1829–1835. DOI: 10.2136/sssaj1999.6361829x.

Neufang, L., Auerswald, K., Flacke, W., 1989a. Automatisierte Erosionsprognose und Gewässerverschmutzungskarten mit Hilfe der dABAG. Ein Beitrag zur standortgerechten Bodennutzung. Bayerisches Landwirtschaftliches Jahrbuch, 66, 771 789. Online available at: http://gruenland.wzw.tum.de/fileadmin/auerswald/1989_Neufang_ByLwJb.pdf (last access: 24 July 2018).

Neufang, L., Auerswald, K., Flacke, W., 1989b. Räumlich differenzierende Berechnung großmaßstäblicher Erosionsprognosekarten – Anwendung der dABAG in der Flurbereinigung und Landwirtschaftsberatung. Zeitschrift für Kulturtechnik und Landentwicklung, 30, 233 241. Online available at: http://gruenland.wzw.tum.de/fileadmin/auerswald/1989_Neufang-KuL.pdf (last access: 24 July 2018).

Oldeman, L.R., 1994. The global extent of soil degradation. In: Greenland, D.J., Szabolcs, I., editors. Soil resilience and sustainable land use. Wallingford: CAB International, 99-118.

Oldeman, L.R., Hakkeling, R.T.A., Sombroek, W.G., 1991. World map of the status of human-induced soil degradation. An explanatory note. ISRIC: Wageningen.

Overeem, A., Leijnse, H., Uijlenhoet, R., 2018. Rainfall monitoring using microwave links from cellular communication networks: The Dutch experience. IEEE Statistical Signal Processing Workshop (SSP), Freiburg, 110-114. DOI: 10.1109/SSP.2018.8450708.

Panagos, P., Ballabio, C., Borrelli, P., Meusburger, K., Klik, A., Rousseva, S., Tadic, M., Michaelides, S., Hrabalíková, M., Olsen, P., Aalto, J., Lakatos, M., Rymszewicz, A., Dumitrescu, A., Beguería, S., Alewell, C., 2015. Rainfall erosivity in Europe. Science of the Total Environment, 511, 801-814. DOI: 10.1016/j.scitotenv.2015.01.008.

Panagos, P, Borrelli, P., Spinoni, J., Ballabio, C., Meusburger, K., Beguería, S., Klik, A., Michaelides, S., Petan, S., Hrabalíková, M., Olsen, P., Aalto, J., Lakatos, M., Rymszewicz, A., Dumitrescu, A., Tadic, M.P., Diodato, N., Kostalova, J., Rousseva, S., Banasik, K., Alewell, C., 2016. Monthly rainfall erosivity: Conversion factors for different time resolutions and regional assessments. Water, 8, 1-18- DOI: 10.3390/w8040119.

Park, Y.S., Kim, J., Kim, N.W., Kim, S.J., Joen, J.-H., Engel, B.A., Jang, W., Lim, K.J., 2010. Development of new *R*, *C* and SDR modules for the SATEEC GIS system. Computers & Geosciences, 36, 726-734. DOI: 10.1016/j.cageo.2009.11.005.

Paulat, M., Frei, C., Hagen, M., Wernli, H., 2008. A gridded dataset of hourly precipitation in Germany: its construction, climatology and application. Meteorologische Zeitschrift, 17, 719–732. DOI: 10.1127/0941-2948/2008/0332.

Pedersen, L., Jensen, N.E., Christensen, L.E., Madsen, H., 2010. Quantification of the spatial variability of rainfall based on a dense network of rain gauges. Atmospheric Research, 95, 441–454. DOI: 10.1016/j.atmosres.2009.11.007.

Peleg, N., Ben-Asher, M., Morin, E., 2013. Radar subpixel-scale rainfall variability and uncertainty: lessons learned from observations of a dense rain-gauge network. Hydrology and Earth System Sciences, 17, 2195-2208. DOI: 10.5194/hess-17-2195-2013.

Pebesma, E.J., 2004. Multivariable geostatistics in S: the gstat package. Computers & Geosciences, 30, 683-691. DOI: 10.1016/j.cageo.2004.03.012.

Pimentel, D., 2006. Soil erosion: A food and environmental threat. Environment, Development and Sustainability, 8, 119-137. DOI: 10.1007/s10668-005-1262-8.

Pimentel, D., Harvey, C., Resosudarmo, P., Sinclair, K., Kurz, D., McNair, M., Crist, S., Shpritz, L., Fitton, L., Saffouri, R., Blair, R., 1995. Environmental and economic costs of soil erosion and conservation benefits. Science, New Series, 267, 1117-1123. DOI: 10.1126/science.267.5201.1117.

Poesen, J., 2017. Soil erosion in the Anthropocene: Research needs. Earth Surface Processes and Landforms, 43, 64-84. DOI: 10.1002/esp.4250.

Poesen, J., Vandaele, K., van Wesemael, B., 1996. Contribution of gully erosion to sediment production in cultivated lands and rangelands. International Association of Hydrological Sciences, 236, 251-266.

Posthumus, H., Deeks, L.K., Fenn, I., Rickson, R.J., 2011. Soil conservation in two English catchments: Linking soil management with policies. Land Degradation and Development, 22, 97-110. DOI: 10.1002/ldr.987.

Prasuhn, V., Liniger, H., Gisler, S., Herweg, K., Candinas, A., Clément, J.-P., 2013. A high-resolution soil erosion risk map of Switzerland as strategic policy support system. Land Use Policy, 32, 281-291. DOI: 10.1016/j.landusepol.2012.11.006.

R Core Team, 2015. R: A language and environment for statistical computing. R Foundation for Statistical Computing, Vienna, Austria http://www.R-project.org/.

Renard, K.G., Foster, G.R., Weesies, G.A., McCool, D.K., Yoder, D.C., 1997. Predicting soil erosion by water: a guide to conservation planning with the Revised Universal Soil Loss Equation (RUSLE). In: Agriculture Handbook Issue 703. US Department of Agriculture: Washington, DC.

Renard, K.G., Simanton, J.R., 1975. Thunderstorm precipitation effects on rainfall-erosion index of the universal soil loss equation. Hydrology and Water Resources in Arizona and Southwest, 5, 47-55.

Renard, K.G., Yoder, D.C., Lightle, D.T., Dabney, S.M., 2011. Universal Soil Loss Equation and Revised Universal Soil Loss Equation. Chap. 8 in: Handbook of Erosion Modelling, Morgan, R.P.C. and Nearing, M. (Eds.), 137-167. Wiley-Blackwell, 401 pp. Online available at: www.tucson.ars.ag.gov/unit/publications/ASPFiles/listing.asp (last access: 2 November 2018).

Risal, A., Lim, K.J., Bhattarai, R., Yang, J.E., Noh, H., Pathak, R., Kim, J., 2018. Development of web-based WERM-S module for estimating spatially distributed rainfall erosivity index (EI30) using RADAR rainfall data. Catena, 161, 37-49. DOI: 10.1016/j.catena.2017.10.015.

Rogler, H., Schwertmann, U., 1981. Erosivität der Niederschläge und Isoerodentkarte Bayerns. Zeitschrift für Kulturtechnik und Flurbereinigung 22, 99-112.

Routschek, A., Schmidt, J., Kreienkamp, F., 2014. Impact of climate change on soil erosion – A high-resolution projection on catchment scale until 2100 in Saxony/Germany. Catena, 121, 99-109. DOI: 10.1016/j.catena.2014.04.019.

Rüttimann, M., Schaub, D., Prasuhn, V., Rüegg, W., 1995. Measurement of runoff and soil erosion on regularly cultivated fields in Switzerland – some critical considerations. Catena, 25, 127-139. DOI: 10.1016/0341-8162(95)00005-D.

Sauerborn, P., 1994. Die Erosivität der Niederschläge in Deutschland. Ein Beitrag zur quantitativen Prognose der Bodenerosion durch Wasser in Mitteleuropa. Bonner Bodenkundliche Abhandlungen 13.

Schmidt, J., 1991. A mathematical model to simulate rainfall erosion. Catena Supplement, 19, 101-109.

Schmidt, J., 1996. Entwicklung und Anwendung eines physikalisch begründeten Simulationsmodells für die Erosion geneigter landwirtschaftlicher Nutzflächen. Berliner Geographische Abhandlungen, 61, 1-148.

Schwertmann, U., Vogl, W., Kainz, M., 1990. Bodenerosion durch Wasser: Vorhersage des Abtrags und Bewertung von Gegenmassnahmen, 2nd Edition. Ulmer, Stuttgart.

Silverman, B.W., 1986. Density estimation for statistics and data analysis. In: Monographs on Statistics and Applied Probability. Chapman and Hall, London.

Steinhoff-Knopp, B., Burkhard, B., 2018. Soil erosion by water in Northern Germany: long-term monitoring results from Lower Saxony. Catena, 165, 299-309. DOI: 10.1016/j.catena.2018.02.017.

Stewart, E.J., 1989. Areal reduction factors for design storm construction: Joint use of raingauge and radar data. In: New directions for surface water modeling. Proceedings of the Baltimore Symposium, May 1989. International Association of Hydrological Sciences, 181, 31-40.

Stewart, B.A., Woolhiser, D.A., Wischmeier, W.H., Caro, J.H., and Frere, M.H., 1976. Control of water pollution from cropland, Vol. II, an overview. U.S. Department of Agriculture and Environmental Protection Agency, ARS-H-5-2. Washington, D.C.

Stoate, C., Boatman, N.D., Borralho, R.J., Rio Carvalho, C., de Snoo, G.R., Eden, P., 2001. Ecological impacts of arable intensification in Europe. Journal of Environmental Management 63, 337-365. DOI: 10.1006/jema.2001.0473.

Treisch, M., Brandhuber, R., 2012. Neuberechnung des Erosionsatlas von Bayern. Tagungsband zu den 7. Marktredwitzer Bodenschutztagen, S. 185-189. Online available at: https://www.lfu.bayern.de/boden/bodenschutztage/doc/mbt_2012.pdf (last access: 20 November 2018).

Twardosz, R., 2007. Diurnal variation of precipitation frequency in the warm half of the year according to circulation types in Kraków, South Poland. Theoretical and Applied Climatology, 89, 229–238. DOI: 10.1007/s00704-006-0268-y.

Van Rompaey, A.J.J., Verstraeten, G., Van Oost, K., Govers, G., Poesen, J., 2001. Modelling mean annual sediment yield using a distributed approach. Earth Surface Processes Landforms, 26, 1221-1236. DOI: 10.1002/esp.275.

Verheijen, F.G.A., Jones, R.J.A., Rickson, R.J., Smith, C.J., 2009. Tolerable versus actual soil erosion rates in Europe. Earth-Science Reviews, 94, 23-28. DOI: 10.1016/j.earscirev.2009.02.003.

Verstraeten, G., Poesen, J., Demarée, G., Salles, C., 2006a. Long-term (105 years) variability in rain erosivity as derived from 10-min rainfall depth data for Ukkel (Brussels, Belgium): Implications for assessing soil erosion rates. Journal of Geophysical Research, 111. DOI: 10.1029/2006JD007169.

Verstraeten, G., Poesen, J., Gillijns, K., Govers, G., 2006b. The use of riparian vegetated filter strips to reduce river sediment loads: an overestimated control measure? Hydrological Processes, 20, 4256-4267. DOI: 10.1002/hyp.6155.

Vieira, D.A.N., Dabney, S.M., Yoder, D.C., 2014. Distributed soil loss estimation system including ephemeral gully development and tillage erosion. In: Sediment dynamics from the summit to the sea, edited by: Xu, J.Y, Allison, M.A., Bentley, S.J., Collins, A.L., Erskine, W.D., Golosov, V., Horowitz, A.J., Stone, M., IAHS Publication, 367, 80-86. DOI: doi:10.5194/piahs-367-80-2015.

Von Werner, M., 1995. GIS-orientierte Methoden der digitalen Reliefanalyse zur Modellierung von Bodenerosion in kleinen Einzugsgebieten. Dissertation, Freie Universität Berlin, Berlin.

Wagner, A., Seltmann, J., Kunstmann, H., 2012. Joint statistical correction of clutters, spokes and beam height for a radar derived precipitation climatology in southern Germany. Hydrological Earth System Sciences, 16, 4101-4117. DOI: 10.5194/hess-16-4101-2012.

Weigl, E., 2018. RADOLAN. Änderungen der operationellen Routine. Version 1.6.6. Stand: 25. April 2018. Deutscher Wetterdienst, Hydrometeorologie. Online available at: https://www.dwd.de/DE/leistungen/radolan/radolan_info/radolan_aenderungen_pdf.pdf?__blob=publicationFile&v=12 (last access: 19 December 2018).

Weiss, L.L., 1964. Ratio of true to fixed-interval maximum rainfall. Journal of the Hydraulics Division, 90, 77-82.

Wendt, R.C., Alberts, E.E., Hjelmfelt, A.T.Jr., 1986. Variability of runoff and soil loss from fallow experimental plots. Soil Science Society of America Journal, 50, 730-736.

Williams, J.R., Renard, K.G., Dyke, P.T., 1983. EPIC: a new method for assessing erosion's effect on soil productivity. Journal of Soil and Water Conservation, 38, 381-383.

Williams, R.G., Sheridan, J.M., 1991. Effect of rainfall measurement time and depth resolution on EI calculation. Transactions of the ASAE, 34, 402-406.

Winterrath, T., Brendel, C., Hafer, M., Junghänel, T., Klameth, A., Lengfeld, K., Walawender, E., Weigl, E., Becker, A., 2018a. RADKLIM Version 2017.002: Reprozessierte, mit Stationsdaten angeeichte Radarmessungen (RADOLAN), Niederschlagsstundensummen (RW). DOI: 10.5676/DWD/RADKLIM_RW_V2017.002.

Winterrath, T., Brendel, C., Hafer, M., Junghänel, T., Klameth, A., Lengfeld, K., Walawender, E., Weigl, E., Becker, A., 2018b. RADKLIM Version 2017.002: Reprozessierte, mit Stationsdaten angeeichte Radarmessungen (RADOLAN), 5-Minuten-Niederschlagsraten (YW). DOI: 10.5676/DWD/RADKLIM_YW_V2017.002.

Winterrath, T., Brendel, C., Hafer, M., Junghänel, T., Klameth, A., Walawender, E., Weigl, E., Becker, A., 2017. Erstellung einer dekadischen radargestützten hoch-auflösenden Niederschlagsklimatologie für Deutschland zur Auswertung der rezenten Änderung des Extremverhaltens von Niederschlag. Abschlussbericht. Deutscher Wetterdienst, Offenbach/M. In: Berichte des Deutschen Wetterdienstes, 251. Online available at: http://nbn-resolving.de/urn:nbn:de:101:1-20170908911 (last access: 6 November 2018).

Winterrath, T., Rosenow, W., Weigl, E., 2012. On the DWD quantitative precipitation analysis and nowcasting system for real-time application in German flood risk management. Weather Radar and Hydrology, IAHS Publ. 351, 323-329.

Wischmeier, W.H., 1959. A rainfall erosion index for a universal soil-loss equation. Soil Science Society of America Proceedings, 23, 246-249.

Wischmeier, W.H., 1975. Estimating the soil loss equation's cover and management factor for undisturbed areas. In: Present and prospective technology for predicting sediment yields and sources. Proceedings of the Sediment Yield Workshop, U. S. Dept. of Agric., Sediment. Lab., Oxford, Miss., U. S. Agr. Res. Serv., ARS-S-40, 118-124.

Wischmeier, W.H., Johnson, C.B., Cross, B.V., 1971. A soil erodibility nomograph for farmland and construction sites. Journal of Soil and Water Conservation, 26, 189-193.

Wischmeier, W.H., Smith, D.D., 1958. Rainfall energy and its relationship to soil loss. Transactions American Geophysical Union, 39, 285-291.

Wischmeier, W.H., Smith, D.D., 1965. Rainfall-erosion losses from cropland east of the Rocky Mountains. Guide for selection of practices for soil and water conservation. Agricultural Handbook, 282.

Wischmeier, W.H., Smith, D.D., 1978. Predicting rainfall erosion losses: a guide to conservation planning. Agriculture Handbook, 537. US Department of Agriculture: Washington, DC.

Woodward, D.E., 1999. Method to predict cropland ephemeral gully erosion. Catena, 37, 393-399. DOI: 10.1016/S0341-8162(99)00028-4.

Yeboah, F.K., Lupi, F., Kaplowitz, M.D., 2015. Agricultural landowners' willingness to participate in a filter strip program for watershed protection. Land Use Policy, 49, 75-85. DOI: 10.1016/j.landusepol.2015.07.016.

Yin, S., Xie, Y., Liu, B., Nearing, M.A., 2015. Rainfall erosivity estimation based on rainfall data collected over a range of temporal resolutions. Hydrology and Earth System Sciences, 19, 4113-4126. DOI: 10.5194/hess-19-4113-2015.

Yin, S., Xie, Y., Nearing, M.A., Wang, C., 2007. Estimation of rainfall erosivity using 5- to 60-minute fixed-interval rainfall data from China. Catena, 70, 306-312. DOI: 10.1016/j.catena.2006.10.011.

Young, R.A., Onstad, C.A., Bosch, D.D., Anderson, W.P., 1989. AGNPS: a nonpoint-source pollution model for evaluating agricultural watersheds. Journal of Soil and Water Conservation, 44, 168-173.

Zhu, Q., Yang, X., Yu, B., Tulau, M., McInnes-Clarke, S., Nolan, R.H., Du, Z., Yu, Q., 2018. Estimation of event-based rainfall erosivity from radar after wildfire. Land Degradation and Development, 1-16. DOI: 10.1002/ldr.3146.

Zingg, A.W., 1940. Degree and length of land slope as it affects soil loss in runoff. Agricultural Engineering, 21, 59-64.